frontiers | Frontiers in Marine Science

TYPE Original Research
PUBLISHED 12 January 2023
DOI 10.3389/fmars.2022.1033381

OPEN ACCESS

EDITED BY
Clara F. Rodrigues,
University of Aveiro, Portugal

REVIEWED BY
Jeroen Ingels,
Florida State University, United States
Maickel Armenteros,
Institute of Marine Science and Limnology, National Autonomous University of Mexico, Mexico

*CORRESPONDENCE
Joan M. Bernhard
jbernhard@whoi.edu

SPECIALTY SECTION
This article was submitted to Deep-Sea Environments and Ecology, a section of the journal Frontiers in Marine Science

RECEIVED 31 August 2022
ACCEPTED 02 December 2022
PUBLISHED 12 January 2023

CITATION
Bernhard JM, Nomaki H, Shiratori T, Elmendorf A, Yabuki A, Kimoto K, Tsuchiya M and Shimanaga M (2023) Hydrothermal vent chimney-base sediments as unique habitat for meiobenthos and nanobenthos: Observations on millimeter-scale distributions. *Front. Mar. Sci.* 9:1033381. doi: 10.3389/fmars.2022.1033381

Hydrothermal vent chimney-base sediments as unique habitat for meiobenthos and nanobenthos: Observations on millimeter-scale distributions

Joan M. Bernhard[1]*, Hidetaka Nomaki[2], Takashi Shiratori[3,4], Anastasia Elmendorf[1], Akinori Yabuki[3], Katsunori Kimoto[3], Masashi Tsuchiya[3] and Motohiro Shimanaga[5]

[1]Woods Hole Oceanographic Institution, Geology & Geophysics Department, Woods Hole, MA, United States, [2]Institute for Extra-cutting-edge Science and Technology Avant-garde Research (X-star), Japan Agency for Marine-Earth Science and Technology (JAMSTEC), Yokosuka, Japan, [3]Research Institute for Global Change (RIGC), Japan Agency for Marine-Earth Science and Technology (JAMSTEC), Yokosuka, Japan, [4]Faculty of Life and Environmental Sciences, University of Tsukuba, Tennodai, Tsukuba, Ibaraki, Japan, [5]Aitsu Marine Station, Kumamoto University, Kumamoto, Japan

Hydrothermal vents are critical to marine geochemical cycling and ecosystem functioning. Although hydrothermal vent-associated megafauna and chemoautotrophic prokaryotes have received extensive dedicated study, smaller hydrothermal vent-associated eukaryotes such as meiofauna and nanobiota have received much less attention. These communities comprise critical links in trophic flow and carbon cycling of other marine habitats, so study of their occurrence and role in hydrothermal vent ecosystems is warranted. Further, an understudied vent habitat is the thin sediment cover at the base of hydrothermal vent chimneys. An initial study revealed that sediments at the base of vent chimneys of the Izu-Ogawasara Arc system (western North Pacific) support metazoan meiofauna, but very little is known about the taxonomic composition and abundance of the meiobenthic protists and nanobiota, or their millimeter-scale distributions. Using the Fluorescently Labeled Embedded Coring method (FLEC), we describe results on meiofaunal and nanobiota higher-level identifications, life positions and relative abundances within sediments from three habitats (base of vent chimneys, inside caldera but away from chimneys, and outside caldera) of the Myojin-Knoll caldera and vicinity. Results suggest that the chimney-base community is unique and more abundant compared to non-chimney associated eukaryotic communities. Supporting evidence (molecular phylogeny, scanning and

transmission electron microscopy imaging) documents first known hydrothermal-vent-associated occurrences for two protist taxa. Collectively, results provide valuable insights into a cryptic component of the hydrothermal vent ecosystem.

KEYWORDS

meiofauna, sediment micro-fabric, microscale distribution, benthic foraminifera, protist, Ciliophora, Sessilida peritrich, Myojin Knoll Caldera

1 Introduction

In the food-limited deep sea, hydrothermal vents are important features because they provide the geochemical conditions to support a chemosynthesis-based ecosystem. Such chemosynthetic hydrothermal vent ecosystems often include charismatic megafauna such as siboglinid tube worms and large mussels, which typically harbor microbial symbionts that are critical to each host's success (e.g., Van Dover, 2000). Such megafauna have received intensive dedicated study since the discovery of hydrothermal vents in the late 1970s. In addition to the megafauna, hydrothermal vents also support macrofauna that can be highly abundant; such vent-associated organisms include, e.g., stalked barnacles, gastropods, and polychaetes. A plethora of novel macrofaunal and megafaunal species have been described from hydrothermal vent habitats over recent decades (e.g., gastropoda; Chen et al., 2019).

Far fewer studies have focused on the smaller organisms associated with hydrothermal vents. Metazoan meiofauna such as nematodes, copepods, and ostracods have been found in vent habitats, sometimes in considerable abundance (Uejima et al., 2017). While some evidence suggest that certain nematodes are endemic to hydrothermal vents due to their higher abundance around higher temperature and association with chemosynthetic microorganisms (Zeppilli et al., 2019), other investigations have found little evidence for endemicity in the nematode vent community (Vanreusel et al., 1997; Zekely et al., 2006a; Zeppilli et al., 2014). Some hydrothermal-vent copepods may be endemic because the Dirivultidae family is thought to be isolated to those habitats (Zekely et al., 2006b; Sarrazin et al., 2015; Senokuchi et al., 2018; Uyeno et al., 2018; Zeppilli et al., 2018). Other reports of dirivultid copepods indicate, however, they can also occur in non-vent hard-substrate habitats such as basalts lacking sediment cover (e.g., Gollner et al., 2010b). Certain ostracods are thought to be endemic to hydrothermal vents (Tanaka and Yasuhara, 2016).

Protists, single-cell eukaryotes that are generally considered nanobiota (e.g., euglenoid flagellates, ciliates) or meiofauna (i.e., foraminifera), inhabiting hydrothermal vent habitats have received less dedicated study. Because protists are an important link in the transfer of carbon to higher tropic levels (e.g., Nomaki et al., 2008), further knowledge about their occurrence and activity in hydrothermal vent habitats will contribute to our overall understanding of the entire hydrothermal vent ecosystem. Prior contributions often assessed vent-associated eukaryotic diversity using rRNA gene sequencing of environmental samples (e.g., Edgcomb et al., 2002; López-García et al., 2003; Murdock and Juniper, 2019). Unfortunately, because these contributions were based on extracted DNA, it is technically impossible to distinguish if the source was active or inactive cells. The sequences that came from the overlying water column could not be eliminated, either. Results from a study that extracted RNA suggest ciliates are well represented in many vents (e.g., Guaymas) and that they may not be vent-endemic (Coyne et al., 2013).

Studies of foraminifera, which are rhizarian protists, suggest that they typically occur at hydrothermal vents (Brönnimann et al., 1989; Jonasson and Schroeder-Adams, 1996; Gollner et al., 2007) generally in low abundance with occasional abundances as high as 9.4 individuals 10 cm^{-2} in bare basalt communities (Gollner et al., 2010b), where they typically occur as encrusting agglutinated forms. While few published datasets exist, foraminiferal abundances in vent habitats seem to be patchy (Gollner et al., 2007; Gollner et al., 2010b). One species, *Abyssotherma pacifica*, is thought to be endemic to vent regions (Brönnimann et al., 1989; Lee et al., 1991), although its sequence has never been obtained for comparison to other foraminiferal populations. Typically, foraminifera are missed by early environmental sequencing studies because the barcode gene sequences (e.g., 18S rRNA gene) of foraminifera are too divergent to be amplified *via* PCR with universal primers. Thus, many prior studies based on sequencing of hydrothermal vent samples are not expected to provide realistic data on this taxon.

Hydrothermal vent habitats are diverse, including the iconic metal-rich mineral "chimneys" and large accumulations of "monoculture" megafaunal taxa such as Alvinellid polychaetes, giant tubeworms, *Calyptogena* clams, or Bathymodiolid mussels,

typically congregated around emission sites of varied intensities. One hydrothermal vent habitat that has received very little study to date is the sedimented debris that can accumulate at the base of hydrothermal vent chimneys. Typically, these areas have very thin (several to 10s cm thick) sedimentary cover, making them a challenge to sample quantitatively. A recent study showed that abundances of metazoan meiofauna living in such sediments at the base of hydrothermal vent chimneys can be more abundant than those inhabiting nearby non-vent sediments (Uejima et al., 2017). Nomaki et al. (2019) reported a considerable abundance of a single agglutinated foraminiferal species, *Pelosina* sp., on the surface of chimney-base sediments at a site south of Japan. To our knowledge, additional information on the attributes of foraminiferal communities or other protists from the base of hydrothermal vent chimneys have not been reported in the literature.

Furthermore, nothing is known regarding the fine-scale distributions (i.e., millimeter scale) of meiofauna and nanobiota in chimney-base sediment deposits. It is possible these benthos congregate at the sediment surface to utilize organics raining down from the chimney above, while it is also possible that diffuse, subsurface flow through the chimney wall is exploited by the benthos deeper in the sediment column. To elucidate faunal distributions on sub-millimeter scales within sediments, we used a method that preserves active organisms within sediment cores at the time of fixation. Using this Fluorescently Labeled Embedded Core method (FLEC; Bernhard and Bowser, 1996; Bernhard et al., 2003), we identified enzymatically active, morphologically distinct protists and metazoan meiofauna within the understudied hydrothermal vent chimney-base sediments and determined their millimeter-scale distributions with respect to the sediment-water interface.

Our objective was to investigate how sediment and fauna at the base of hydrothermal vent chimneys differ from sediments of surrounding habitats. We hypothesized that the sedimentary habitat at the base of hydrothermal vent chimneys has a unique and relatively abundant community, potentially linked to the detritus fall from the chimney surface and associated microorganisms living on the vent chimney surface proper. For that purpose, we performed microCT scanning to demonstrate differences in sediment grain composition, organic matter analyses (data reported in Nomaki et al., 2019), and mm-scale taxon distribution of enzymatically active organisms to reveal how living individuals were distributed and oriented with respect to the sediment-water interface where detritus falls arrived. Additionally, we performed ultrastructural analysis on one foraminifer to independently demonstrate its viability as well as to survey for any cellular adaptations that are often noted in vent-associated metazoa. DNA sequencing helped identify an unexpected ciliate morphogroup that may have a unique ecological adaptation(s) to this unique habitat.

2 Materials and methods

2.1 Study site

Myojin Knoll Caldera is located in the Izu-Ogasawara Arc of the western North Pacific Ocean (Figure 1). The Knoll is one of three calderas occurring in close proximity in this island-arc setting. Myojin Knoll has active hydrothermal vents (e.g., Tsunogai et al., 2000; Honsho et al., 2016), with venting fluids emanating the Kuroko-type polymetallic sulfide chimneys at ~287°C (Iizasa et al., 1999). The community of Myojin Knoll has received considerable study, especially for metazoan macro- and megafauna (Sasaki et al., 2010; Yorisue et al., 2016; Koito et al., 2018; Watanabe et al., 2019). Metazoan meiofauna from vent chimney walls have also received dedicated study at

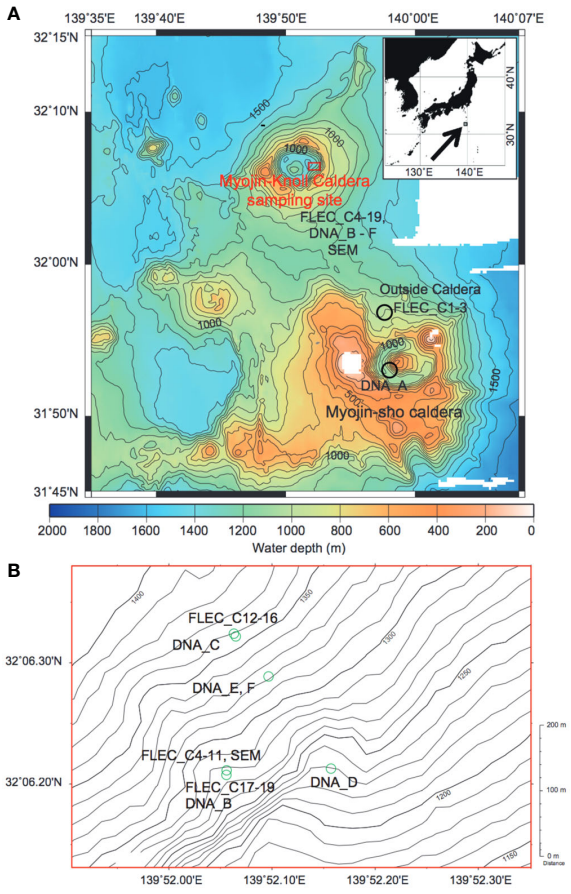

FIGURE 1
Maps showing the collection areas. **(A)** The Izu-Ogasawara Arc region, showing location of Myojin Knoll and Myojin-Sho Calderas in addition to sample sites outside Myojin Knoll Caldera. Inset: Index map showing location of A with respect to Japan. Contours in 100-m increments (modified from Nomaki et al., 2019). **(B)** Enlargement of area inside Myojin-Knoll showing locations of chimney-associated and non-chimney caldera samples. Contours in 10-m increments.

Myojin Knoll (Uejima et al., 2017; Senokuchi et al., 2018; Uyeno et al., 2018). Additionally, the metazoan meiofauna have been documented from the sediments at the base of Myojin Knoll chimneys and nearby habitats (Setoguchi et al., 2014; Uejima et al., 2017), at ≥2-cm depth resolution.

2.2 Sampling

We sampled sediments at the base of the Daimyojin Chimney of Myojin Knoll Caldera, at the base of an unnamed small chimney also in the Myojin Knoll Caldera, as well as in the same caldera but away from the chimneys and outside the caldera (non-vent site; Figure 1). Thus, we sampled sediments from three habitats: chimney base, inside the caldera removed from the chimney/venting (i.e., ~80 m distant), and outside the caldera, approximately 11 km away. We also sampled the Myojin Knoll chimney wall detritus for selected analyses. The water depths of sampling sites ranged from 994 to 1399 m (Table 1).

Sediment samples were collected using ROV *Hyperdolphin* on R/V *Natsushima* cruise NT13-09 from 20-29 April 2013. Specifically, sediment cores were collected during *Hyperdolphin* dives #1517, 1519, and 1520. Sites were selected based on the appearance of sediments in the regions of interest. At each selected site, 8.2-cm inner diameter pushcores (H-cores, Table 1) were collected using the ROV manipulator. After pushcores were aboard the ship, they were subcored in the cold room (4°C) for life-position analyses (i.e., FLEC) as described below. Additional pushcore sediment samples obtained with the ROV were preserved in 99.9% ethanol as soon as possible upon sample recovery; an aliquot of a pushcore taken adjacent to Cores 8 and 9 was the source of select foraminifera for morphological documentation *via* Scanning Electron Microscopy (SEM).

Sediment samples for sequencing were collected in pushcores *via* ROV manipulator on R/V *Natsushima* cruise NT12-10 (April 2012) and R/V *Shinsei-maru* cruise KS18-03 (April 2018; Table 1 samples with letter designations). Most pushcores had an inner diameter of 8.2 cm (H type, Table 1) while some had an inner diameter of 4.0 cm (S-cores). In one case, the sediment veneer was too thin to core due to underlying rock and/or concretions, so the surficial ~2-3 cm of sediment was collected *via* scoop (sample D, Table 1). Additionally, some samples intended for sequencing were collected *via* suction sampler (Table 1, Samples E, F), which allowed sampling of the chimney wall. The "slurp gun" suction sampler was equipped with a 30-µm mesh at the outlet of each of six sampling chambers, so bacterial mats, detritus, and meiofauna could be obtained from the vertical surface of the vent chimney.

2.2.1 Sediment fabric

Sediment fabric of FLEC cores was examined using a micro-focus X-ray computed tomography system (i.e., micro-CT; ScanXmate-DF160TSS105, Comscantecno CO. Ltd., Kanagawa, Japan). The observed settings were X-ray tube voltage of 80 kV, tube current of 30 µA, detector array size of 1024 X 1024, voxel size of 18.8 µm (for entire FLEC core imaging) and 5.7 µm (higher resolution observation of the central part of FLEC), 1500 projections/360°, and 10 frames.

2.2.2 *In situ* distributions

The FLEC method (Bernhard and Bowser, 1996; Bernhard et al., 2003) melds sedimentological approaches to assess sediment fabric (Frankel, 1970; Watling, 1988) with use of the fluorogenic probe CellTracker™ Green CMFDA (chloromethyl fluorescein diacetate; Thermo Fisher; hereafter "CTG") to identify active organisms in sediments. The approach has been used in varied natural settings (Bernhard et al., 2003; Bernhard and Buck, 2004; First and Hollibaugh, 2010) and in experiments (Bernhard et al., 2013).

A maximum of five syringe cores (1.5-cm inner diameter) were obtained from each FLEC designated pushcore. Syringe cores were maintained near *in situ* temperature (4°C) and incubated with 1 µM CTG (final concentration) using our standard protocols (e.g., Bernhard et al., 2003). To help preserve foraminiferal reticulopodia, calcium-free seawater was introduced into some of the syringe cores (6, 7, 9, 11, 14, 15, 17, 18; designated with * in Table 1) just before initiation of CTG incubation. After an incubation of at least 12 hours, syringe cores were preserved in 3% TEM-grade glutaraldehyde in 0.1M cacodylic acid (pH 7.2).

At JAMSTEC, syringe cores were perfused in buffer three times and serially dehydrated with ethanol over a period of months. After the third 99.5% ethanol perfusion, syringe cores were perfused twice with acetone, and infiltrated with Spurr's low viscosity resin. After two perfusions of uncatalyzed resin and two subsequent perfusions of catalyzed resin, syringe cores were polymerized at 70°C. Processing of Core 3 through the polymerization step resulted in loss of its core top, thus results from this core are not included in our reporting. In sum, a total of eighteen cores polymerized successfully and were assessed.

At WHOI, polymerized cores were excised from syringe barrels and subsequently processed with a Buehler Isomet slow speed rock saw with water-soluble coolant. After cutting each core at the bottom and ~0.5 cm above the sediment-water interface, each was then sectioned vertically so that approximately 16 vertical (longitudinal) sections of ~1-mm thickness were obtained for each core. The maximum core section length was 3 cm. Prior to examination with epifluorescence microscopy, sections were typically ground briefly with wet sandpaper (800 grit) to polish the section surfaces.

Both sides of each core section were then examined with an epifluorescence-equipped dissecting microscope to identify regions of interest for higher magnification analysis *via*

10.3389/fmars.2022.1033381

TABLE 1 Sample details including samples identification number/letter (1-19 = FLEC; A-F = DNA), date of collection, cruise number, *Hyperdolphin* dive number, coordinates, water depth (m), sample identification, and push-core replicate designation.

Sample ID	Date	Cruise ID	Dive #	Location	Habitat	Latitude (°N)	Longitude (°E)	Water depth	Push Core #	Replicate
1	4/23/2013	NT13-09	HPD 1517	Outside Caldera	Non-vent reference	31 56.820	139 57.588	1002	H-4	A
2					Non-vent reference					B
4	4/26/2013	NT13-09	HPD 1519	Myojin-Knoll Caldera, Daimyojin Chimney	Chimney-base sediment	32 06.226	139 52.052	1269	H-1	A
5					Chimney-base sediment					B
6					Chimney-base sediment					A*
7					Chimney-base sediment					B*
8	4/26/2013	NT13-09	HPD 1519	Myojin-Knoll Caldera, Daimyojin Chimney	Chimney-base sediment	32 06.226	139 52.052	1267	S-Green	A
9					Chimney-base sediment					C*
10	4/26/2013	NT13-09	HPD 1519	Myojin-Knoll Caldera, Daimyojin Chimney	Chimney-base sediment	32 06.226	139 52.052	1267	H-3	B
11					Chimney-base sediment					D*
12	4/28/2013	NT13-09	HPD 1520	Myojin-Knoll Caldera, control site	Caldera control	32 06.331	139 52.062	1354	H-4	A
13					Caldera control					B
14					Caldera control					C*
15					Caldera control					D*
16					Caldera control					E
17	4/28/2013	NT13-09	HPD 1520	Myojin-Knoll Caldera, chimney	Chimney-base sediment	32 06.206	139 52.052	1258	H-5	A*
18					Chimney-base sediment					B*
19					Chimney-base sediment					C

(Continued)

TABLE 1 Continued

Sample ID	Date	Cruise ID	Dive #	Location	Habitat	Latitude (°N)	Longitude (°E)	Water depth	Push Core #	Replicate
SEM	4/26/2013	NT13-09	HPD 1519	Myojin-Knoll Caldera, Daimyojin Chimney	Chimney-base sediment	32 06.226	139 52.052	1269	S-Red	SEM
A	4/25/2012	NT12-10	HPD 1374	Myojin-sho Caldera, control site	Caldera control	31 53.013	139 58.010	994	H-2	
B	4/29/2012	NT12-10	HPD 1377	Myojin-Knoll Caldera, Daimyojin Chimney	Chimney-base sediment	32 06.214	139 52.053	1266	S-4	
C	4/5/2018	KS18-03	HPD 2057	Myojin-Knoll Caldera, control site	Caldera control	32 06.325	139 52.066	1354	H-1	
D	4/4/2018	KS18-03	HPD 2056	Myojin-Knoll Caldera, chimney	Chimney-base sediment	32 06.219	139 52.157	1225	M	
E	4/29/2012	NT12-10	HPD 1377	Myojin-Knoll Caldera, chimney	Chimney-wall detritus	32 06.286	139 52.096	1321	Canister 1	
F	4/29/2012	NT12-10	HPD 1377	Myojin-Knoll Caldera, chimney	Chimney-wall detritus	32 06.286	139 52.096	1321	Canister 2	

*FLEC core incubated in Ca-free seawater prior to fixation.

confocal laser scanning microscopy (CLSM). An Olympus Fluoview 300 CLSM was used to survey both sides of at least 5 core sections per core at both 100× and 200× magnification. The two flank sections near each core edge were not included because of their small width and possible specimen draw down during subcoring and/or perfusions. For a subset of cores, both sides of ≥10 sections were fully examined. The regions deeper than ~1 cm of all cores could not be examined for fluorescent individuals due to presence of widespread non-specific autofluorescence that likely was due to insufficient solution changes in the preparation procedure. Glutaraldehyde can impart dim autofluorescence in the fluorescein emission range.

Brightly fluorescent items were examined closely. Dimly fluorescent objects, which could be dead, were not considered in our analyses. Of brightly fluorescent organisms, all foraminifers were imaged as were all metazoans, except nematodes which were quite abundant in some cores (i.e., cores 4-11, collected from the base of the Daimyojin Chimney) where our counts represent their minimum abundances. Unequivocal flagellates were rarely imaged because flagella were difficult to ascertain; thus, flagellates were not quantified. In some cases nanobiota-sized organisms were clumped, as has been noted previously for some flagellates (e.g., Bernhard et al., 2003); these were often imaged. The sections remain available for additional analyses, as warranted. All CLSM images (i.e., Figures 2–8; Supplementary Figures 2-4) are presented in proper vertical orientation.

2.2.3 Foraminiferal cellular ultrastructure

One CTG-labeled foraminifer that occurred in chimney-base sediments (i.e., FLEC section from Core 6) was selected for further analysis using Transmission Electron Microscopy (TEM). After the specimen was imaged *via* reflected, transmitted and CLSM microscopy, it was excised from the section, mounted on a resin plug, trimmed, and sectioned *via* ultramicrotome (Bernhard and Richardson, 2014). Thin sections (90 nm) were post-stained for 6 minutes in 1% aqueous uranyl acetate and 3 minutes in lead citrate. Sections were examined and imaged with a JEOL JEM-200CX TEM operated at 100 kV at the Marine Biological Laboratory's Central Microscopy Facility (Woods Hole, MA, USA).

2.2.4 SEM observation of foraminifera tests

Specimens of a single common foraminifer were isolated from 99.9% EtOH-fixed chimney-base sediment collected during the NT13-09 cruise. The EtOH-fixed sediments were washed over a 32-μm sieve using filtered (0.2 μm) artificial seawater and transferred to a Petri dish. Foraminiferal specimens were isolated using a Pasteur pipette under a binocular microscope. The specimens were then washed with 0.2-μm filter-sterilized seawater and cleaned with a small brush to remove foreign materials. The specimens were dried at room temperature in preparation for scanning electron microscopy (SEM) observation and then coated with osmium using an osmium plasma coater (OPC80, Filgen, Nagoya, Japan). The

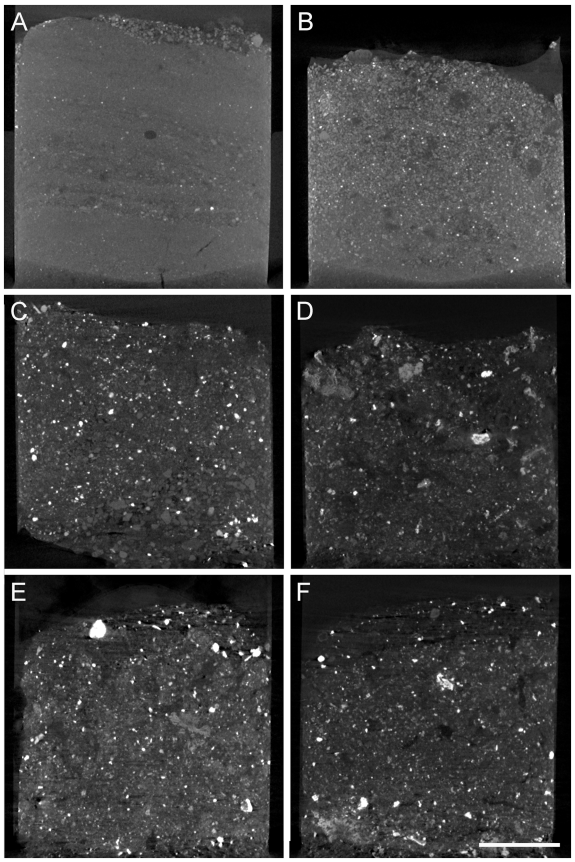

FIGURE 2
Representative vertical cross-section micro-CT scans of FLEC cores from the three habitats. **(A)** Core 2 from outside the caldera. **(B)** Core 14 from inside the caldera but away from the chimneys. **(C)** Core 7 from base of Daimyojin Chimney. **(D)** Core 19 from base of smaller chimney. **(E)** Core 8 from base of Daimyojin Chimney. **(F)** Core 11 from base of the smaller chimney. Scale = 5 mm.

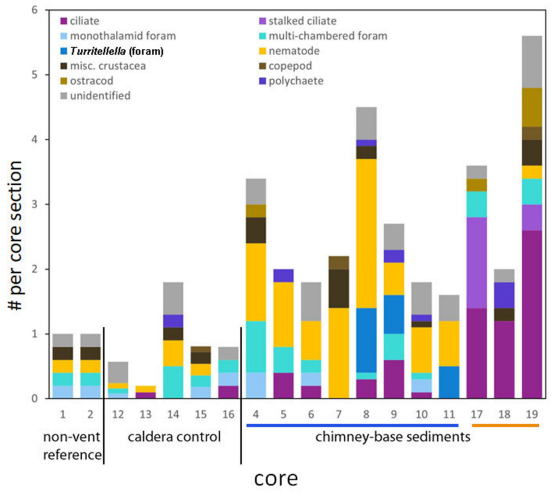

FIGURE 3
Stacked bar graph showing eukaryote abundance by major group/taxa of interest for each core, ordered by habitat. The bars under the x-axis denote the two chimneys: Daimyojin Chimney with >20m height is the blue bar; smaller chimney with ~2m height is the orange bar. Values are standardized per core section. *Turritellella* foraminifer counts are not included in the Multi-chamber foraminifera category. Flagellates not included.

detailed fine structures of the test were observed with a Quanta 450 FEG SEM (FEI, Hillsboro, OR, USA) at an acceleration voltage of 5.0kV. Specimens were imaged with a vCD (low voltage high contrast detector, FEI) camera attached to the E-SEM.

2.2.5 Molecular phylogeny of sediment and chimney-wall detritus Peritrichs

Total DNAs of sediment samples were extracted using ISOIL (Nippon Gene) according to the manufacturer's instructions. The small subunit ribosomal RNA (SSU rRNA) gene sequences of peritrich ciliates were amplified by semi-nested PCR using universal and peritrich-specific primers. The first PCR was performed using oligonucleotide primers EukA [5'-AACCTGGTTGATCCTGCCAGT-3', Medlin et al. (1988)] and Peri1403R [5'-GGGCGRTGTGTACATTTTG-3', Liu and Gong (2012)] under the following conditions: initial denaturation at 94°C for 1 min followed by 35 cycles consisting of a denaturation at 94°C for 30 sec, an annealing at 50°C for 30 sec, and an extension at 72°C for 2 min. An additional extension at 72°C for 7 min was performed at the end of the reaction. PCR products were purified using the Wizard® SV Gel and PCR Clean-Up System (Promega). The second PCR was performed using primers Peri974F [5'-GGAAACTCATCAGGRCAAGAAGATT-3' (Liu and Gong, 2012)] and Peri1403R under the following temperature conditions: initial denaturation at 94°C for 1 min followed by 35 cycles consisting of a denaturation at 94°C for 30 sec, an annealing at 50°C for 30 sec, and an extension at 72°C for 1 min. An additional extension at 72°C for 7 min was performed at the end of the reaction. The second PCR products were electrophoresed to separate expected size (441 bp) fragments. The expected size fragments were cut from the gel and purified using the Wizard® SV Gel and PCR Clean-Up System. Purified second PCR products were cloned using TOPO® TA Cloning Kit for Sequencing (Invitrogen), and each of eight white colonies was screened and sequenced using an ABI PRISM 3730xl Analyzer (Applied Biosystems). The SSU rDNA sequences of peritrichids were deposited in GenBank as LC723767-

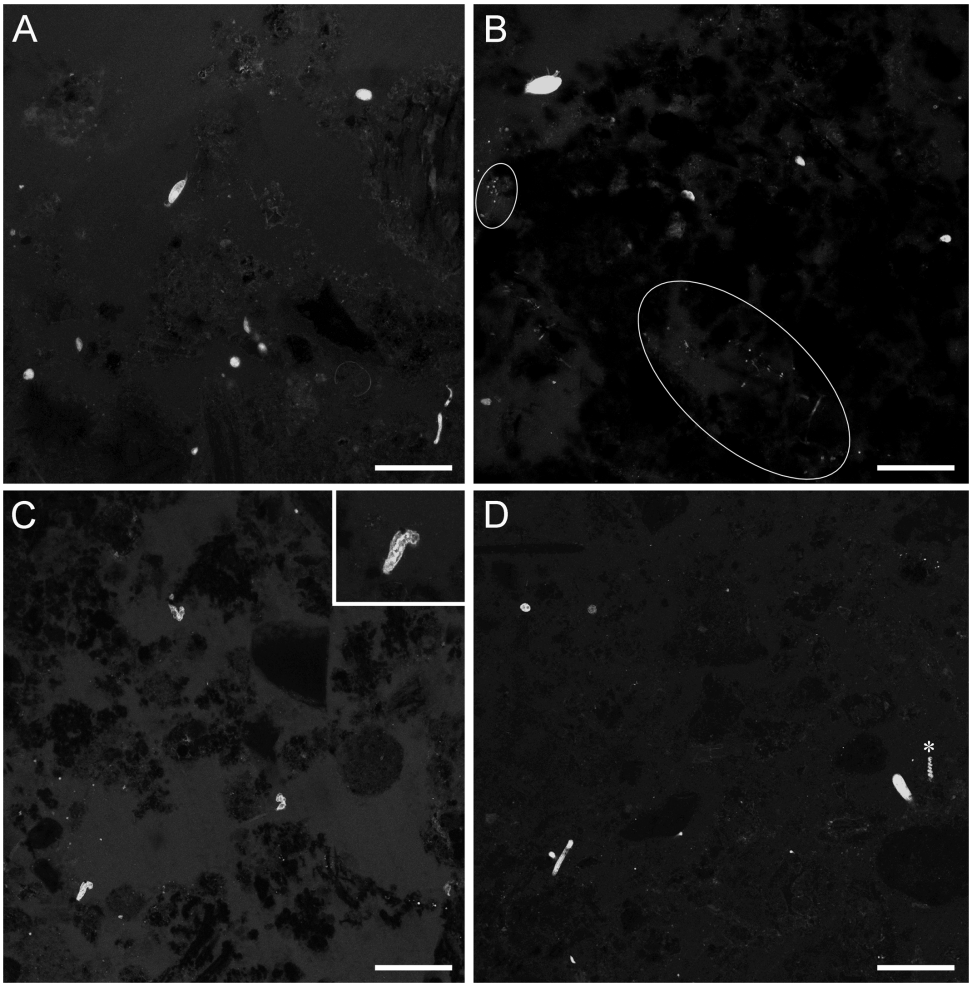

FIGURE 4
LSCM images (z-stacks) of FLEC sections showing overview examples of chimney-base sediments with inhabitants. **(A)** Core 5 showing mixed community of protists and metazoans, ~1mm depth. **(B)** Core 4, ~2 mm depth. **(C)** Core 19 showing three ciliates of similar morphology, ~2 mm depth; Inset in C shows higher magnification view of one ciliate in C. **(D)** Core 8, ~2 mm depth. White ovals highlight areas with aggregated microbes, **Turritellella*-like foraminifer. Number of images compiled/distance between images (µm): A=43/0.7; B=31/0.7; C= 20/1.4; D=20/1.4; Scales: A,B = 100 µm; C,D = 200 µm.

LC723776. For molecular phylogenetic analysis, we created a dataset that included ten peritrich SSU rRNA gene sequences obtained in this study and 22 related ciliate sequences obtained from the GenBank database. The dataset was automatically aligned using MAFFT (Katoh and Standley, 2013) with the G-INS-i algorithm. The alignment was edited manually using SeaView (Gouy et al., 2010) to remove ambiguously aligned regions. A maximum likelihood (ML) tree was inferred using IQ-TREE v. 1.64.12 (Nguyen et al., 2015) with 100 non-parametric bootstrap replicates. The best-fit model (TPM2u+F+I+G4) that was determined based on the Bayesian information criterion (BIC) was used for the analysis.

3 Results

3.1 Sediment fabric

Micro-CT scans revealed that the sediments of the three habitats noticeably differed (Figure 2). The cores from outside the caldera were fine grained, had slight layering and a slightly coarser-grained surface veneer (Figure 2A). The cores from inside the caldera but afar from the chimneys had slightly coarser grains (Figure 2B) compared to sediments collected outside the caldera, of more heterogenous compositions revealed by wider grayscale range (i.e., degrees of x-ray

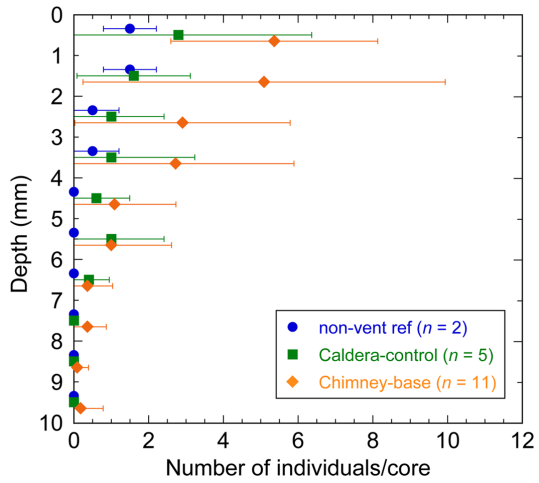

FIGURE 5
Vertical profiles showing the mean abundance of total eukaryotes (minus flagellates) at mm-scale downcore. Means and error bars (1SD) were calculated for each habitat.

attenuation) in the scans. The chimney-base cores (Figures 2C–F) showed no layering, were coarser grained, poorly sorted, and had numerous x-ray opaque grains (white in scans), which are generally considered to be rich in heavy metals (e.g., base and precious metals; Nozaki et al., 2016). In cores collected at the base of the chimneys, sediment grains commonly appeared to have rather angular shapes and/or be composed of crystallites/aggregations (not shown).

3.2 Taxa and their distributions

Fluorescently labeled organisms were found in each FLEC core (n=18), although some cores appeared to contain very few identifiable organisms (Figure 3). In some instances, a fluorescent organism could not be identified, even to phylum level due to, e.g., partial loss of specimen because of sectioning, blurred imaging due to its occurrence deep within a polymerized core section, and/or non-characteristic morphology (e.g., spherical).

High-level taxonomic diversity often varied among cores from the same habitats (Supplementary Table 1). The only groups identified in cores obtained from outside the caldera were foraminifera, nematodes, and crustaceans, typically larvae, while cores from inside the caldera often, but not always, had more phyla. The chimney-associated cores had higher densities of ciliates and meiofauna (Figure 3) compared to non-chimney cores; some of this abundance and diversity was evident in FLEC images (e.g., Figure 4). Foraminifera and nematodes were the most common and widespread taxa, observed in all but one non-chimney core and two chimney-associated cores (Figure 3). The majority of fluorescent eukaryotes occurred in the surface 4 mm (Figure 5). For example, over 80% of the foraminifera occurred in the top 4 mm (Supplementary Figure 1; Supplementary Table 2).

Nematodes were abundant especially in cores from the base of chimneys (Figures 3, 6A–C; Supplementary Table 1), where multiple specimens could occur in close proximity (Figures 6B, C). Based on morphological appearance (specimen diameter, length) in the FLEC sections, the nematodes were likely speciose. Crustaceans, being present mostly as copepods, ostracods, possible nauplii, or unidentifiable forms (Figures 6D–F and Supplementary Figure 2F), were present but uncommon in most of our samples and absent in four chimney-associated cores and three non-chimney cores. What may have been a veliger was present in a chimney-base core (Figure 6G). A tanaid (~820 µm long) occurred about 5 mm below the sediment-water interface in Core 15 (Supplementary Figure 3A), which was from inside the caldera but not near a chimney.

Polychaetes were the largest organisms observed, being up to many mm in length and up to ~640 µm in diameter (Supplementary Figures 3B, C), and noted in five of eleven cores associated with the base of the two different vent chimneys and one of the five non-chimney caldera cores (Figure 3). In Core 18, a large individual was inside its tube (faintly visible in Supplementary Figures 3B, C), while there was no evidence of a tube in the vicinity of a large polychaete in Core 9, although a tube was noted in the microCT scan of this core (not shown). Additional polychaetes occurred, but these were considerably smaller (Supplementary Figure 3D). A structure with apparent radial symmetry may have been a branchial filament of a juvenile *Paralvinella* polychaete (Supplementary Figure 2A) or, potentially a cnidarian; the posterior of a copepod or a putative rotifer was also noted (Supplementary Figure 2B). Other individuals could not be assigned even to phylum (e.g., Supplementary Figures 2C-F) or could have been either a metazoan or protist (Supplementary Figure 2G). In some cases, the unidentifiable specimen could even be observed from both sides of a FLEC section (Supplementary Figures 2D, E).

Ciliates were observed in most chimney-base cores (i.e., 8 of 11 cores) but only in two of the seven cores not associated with chimneys (Figures 3). When present, ciliates appeared to be morphologically diverse (Figures 7, 8). Usually, ciliate morphotypes were only noted once or twice although one morphotype occurred relatively often, especially in Core 19 (Figure 4C) and Core 18 (Figure 7D), which were chimney-base sediments. A second ciliate morphotype was also represented by multiple specimens (n=8). Individuals of this morphotype, which is stalked and morphologically resembling a retracting *Vorticella* (Figure 8), appeared rather commonly in two chimney-base sediment cores (n=6 in Core 17; n=2 in Core 19). The average diameter of these stalked spherical bodies was 22.3 µm (n=6; SD= 2.7 µm). Two additional spheres of similar diameter (22.9 µm) were imaged from Core 17, but these did not

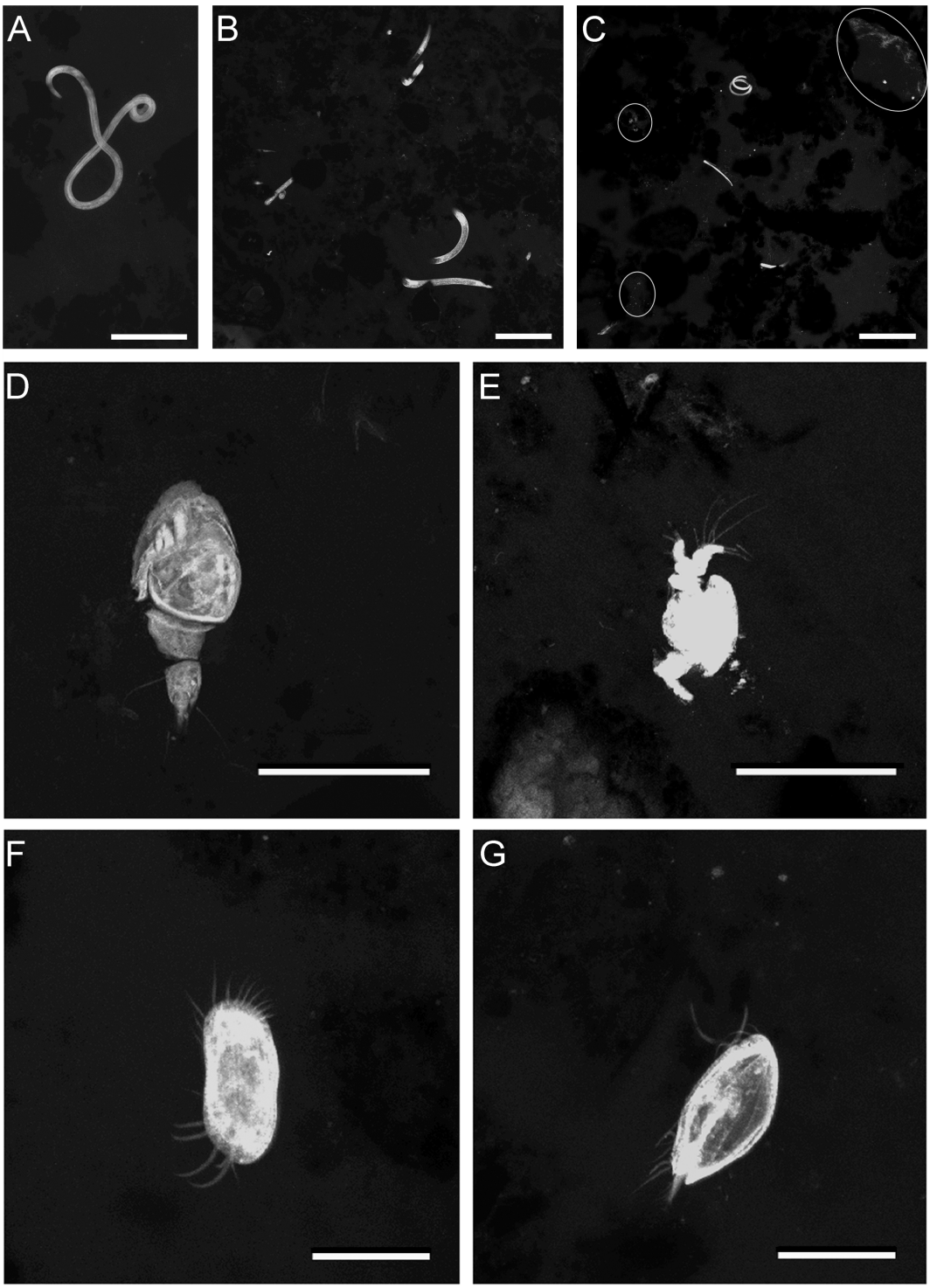

FIGURE 6
FLEC LSCM images (z-stacks) showing metazoan meiofauna from chimney-base sediments. **(A–C)** Nematodes in Core 8. **(A)** Single nematode, ~3mm depth. **(B)** Three nematodes, ~3 mm depth. **(C)** Three nematodes, ~5 mm depth. White outlines highlight microbial aggregations. **(D)** Copepod juvenile, Core 7, ~0.5 mm depth. **(E)** Possible fragment of nauplii, Core 4, 4 mm depth. **(F)** Ostracod (*Argilloecia* sp.)?, Core 19, 3 mm depth. **(G)** Possible bivalve veliger, Core 19, 1 mm depth. White ovals highlight areas with biofilms or aggregated microbes. Number of images compiled/distance between images (µm): **(A)**=71/0.7; **(B)** =29/1.4; **(C)** = 58/1.4; **(D)** = 23/0.7; **(E)** = 24/0.7; **(F)** = 64/0.5; **(G)** = 61/0.5. Scales: **(A, D, E)** = 100 µm; **(B, C)** = 200 µm; **(F, G)** = 50 µm.

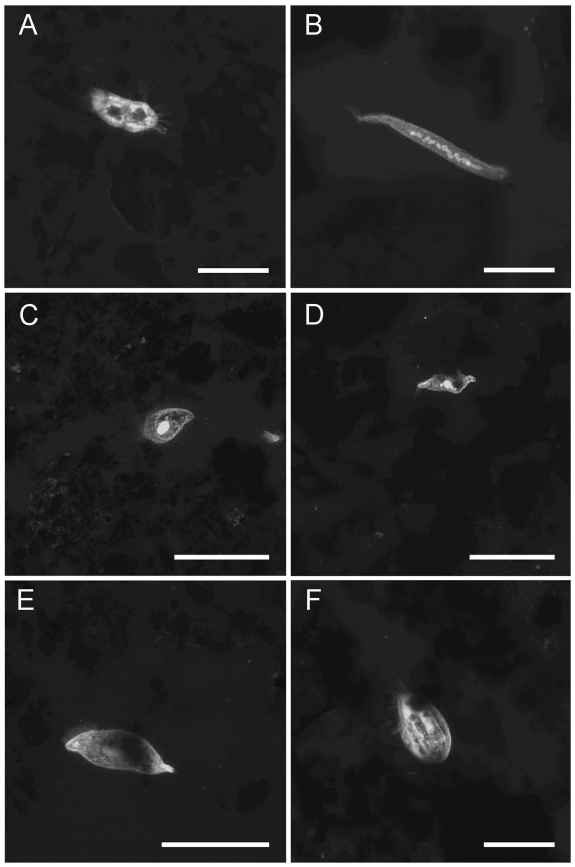

FIGURE 7
LSCM images (z-stacks) of ciliate protists. **(A)** Core 16 (inside caldera removed from chimney), 4mm depth. **(B)** Elongated ciliate with moniliform macronucelus, Core 18 (chimney base), 0.5mm depth. **(C)** Core 19 (chimney base), 1.5mm depth. **(D)** Specimen similar to those in Figure 4C, Core 18 (chimney base), 1mm depth **(E)** Core 17 (chimney base), ~0.5mm depth. **(F)** Core 17 (chimney base), 3mm depth. Number of images compiled/distance between images (µm): **(A)** =27/0.3; **(B)** = 28/0.3; **(C)** = 25/0.7; **(D)** = 31/0.7; **(E)** = 140/0.5; **(F)** = 75/0.3. Scales: **(A, B, F)** = 50 µm; **(C–E)** = 100 µm.

have visible stalks. These could be additional *Vorticella*-like ciliates with an obscured or fully retracted stalk. Although they were confidently identified less often than ciliates, euglenoid flagellates were observed in seven chimney-associated cores but only in two non-chimney cores.

Foraminifera occurred in all three habitats (Figures 3, 9–11; Supplementary Figures 1, 4; Supplementary Table 1). In most cases, any observed foraminiferal morphotype was only noted once or twice. Multi-chambered (globothalamid) foraminifera including trochospiral, uniserial, and biserial forms (Figures 9A–C and Supplementary Figures 4A-D) were more common than monothalamid (single chambered) forms (e.g., Figures 9D, 11), most of which had agglutinated tests. One monothalamid that lacked a mineralized test had the characteristic entosolenial tube of the single-chambered Allogromiidae foraminifers (Supplementary Figures 3E; Meisterfeld et al., 2001; Gooday, 2002). The typical vacuolated cytoplasm fabric (e.g., Bernhard et al., 2006) could be seen in most foraminifers when viewed in FLEC sections (e.g., Figures 9A, D; Supplementary Figures 4A, B, E).

The agglutinated foraminifer *Leptohalysis scottii* was tentatively noted in a non-chimney caldera core from 3-mm depth (Supplementary Figure 4D). We did not observe any calcareous tests associated with any foraminifers, likely because the carbonate dissolved during FLEC processing. As for what were likely calcareous forms, a *Euloxostomum pseudobeyrichi*-like specimen was noted in a chimney core at 4-mm depth (Figure 9A) and biserial *Bolivina*-type specimens were noted in non-chimney base caldera cores from 1- and 4-mm depths, respectively (Supplementary Figures 4B,C).

What appeared to be bacterial biofilms occurred on the surfaces of grains (e.g., Figures 6C, 8A, B and Supplementary Figure 2F) and microbial aggregations appeared in pore interstices (e.g., Figures 4B, 6C, 9A,C, 10A, F). Filamentous microbes were observed in three cores (Cores 4, 5, 17), but in all instances except one, these microbes were not large such as the filamentous colonial *Beggiatoa* and *Thioploca*. All cores containing the filamentous bacteria were from the chimney-base sediment habitat.

3.3 Common foraminiferal morphotypes

Three of the eight cores from the base of Daimyojin Chimney had a distinct foraminifer morphotype (Figures 3, 10) while that helical morphology was not observed in any other cores from any other sites, chimney or non-chimney included. A total of 20 specimens of this foraminifer were observed, with the most being in Core 8 (n=11; Figure 10F), with approximately 11.3 specimens cm^{-3}. Abundance in Cores 9 and 11 were ~6.1 and 3.1 specimens cm^{-3}, respectively. This small morphotype, typically ~20 µm wide and <70 µm long in FLEC sections, appeared to have a proloculus (Figures 10A, B) and, thereafter, a single helical chamber with as many as 13-15 whorls (Figures 10D, E). Longer, more complete specimens had a maximum observed length of ~200 µm (Figure 10D). Because the test (shell) composition of this foraminifer was difficult to discern in FLEC sections, we used Scanning Electron Microscopy to document the test of the same morphotype; such imaging revealed that the test was finely agglutinated (Figure 10E). Thus, this morphotype was tentatively identified as a *Turritellella* species (Höglund, 1947), most likely *T. shoneana* (Siddall, 1878; Hayward et al., 2022). The morphotype could be rather abundant and/or patchy (Figure 10F).

Monothalamid foraminifera in chimney-associated cores (Cores 6, 10) were morphologically similar to *Pelosina* sp., (n=5) which was noted to occur on the sediment surface of other samples collected from the base of Myojin Knoll

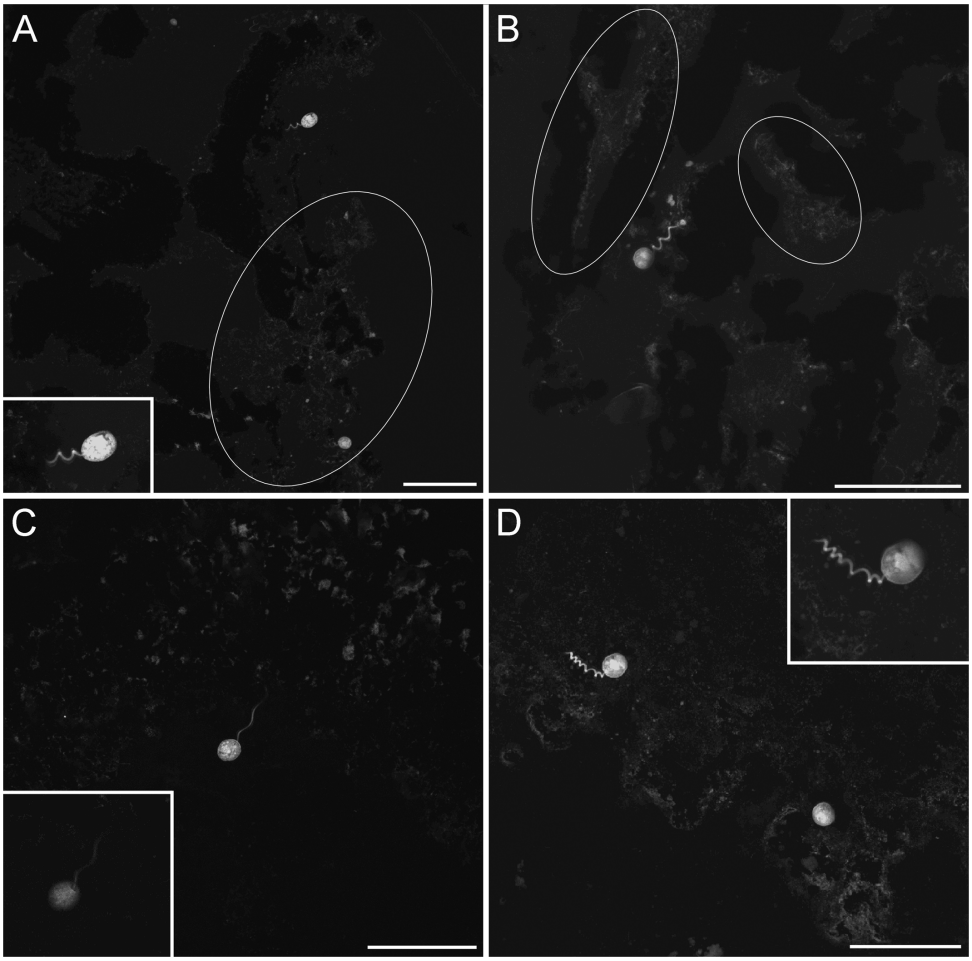

FIGURE 8
LSCM images (z-stacks) of the Vorticellid-like protist, all from chimney base sediments; all specimens in partial retraction. **(A)** Two individuals, occurring at the edge of Core 17, ~1 mm deep. Inset shows higher magnification view of upper specimen. **(B)** Specimen near Core 17 edge, ~0.5 mm depth; white ovals in **(A, B)** highlight well-developed microbe aggregations. **(C)** Core 17, 1 mm deep. Inset reveals attachment between spherical body and stalk. **(D)** One stalked specimen and putative second specimen (lower right) from Core 19, ~0.5 mm depth. Inset shows close up of stalked specimen. Note all Vorticellid-like specimens extend into pore space, not into overlying bottom waters. White ovals highlight areas with well-developed biofilm. Number of images compiled/distance between images (μm): **(A)** = 29/0.7; **(B)** = 49/0.5; **(C)** = 9/0.5; D= 23/0.5; **(A)** Inset=48/0.3; **(C)** Inset=1 slice; **(D)** Inset=37/0.4. Scales: **(A–D)** = 100 μm.

chimneys (Nomaki et al., 2019). One such specimen, which had a thickly agglutinated test, was observed *via* FLEC to be living at the sediment-water interface (Figure 11A). Along with a large nucleus-like structure, the typical vacuolated nature of foraminiferal cytoplasm was evident *via* confocal imaging of this specimen (Figure 11B). Remnant reticulopodia were also visible in confocal images of this specimen (Figures 11C, D). Transmission electron micrographs also showed reticulopodial remnants (Supplementary Figures 5A-C), some with microtubules (Supplementary Figure 5D) as well as abundant vacuoles in the cell body (Supplementary Figures 6A, C-D). Organelles similar in appearance and size to mitochondria were abundant (Supplementary Figure 6A); these had faint double membranes and cristae (Supplementary Figure 6B). Golgi were well preserved and rather abundant (Supplementary Figure 6C). Endoplasmic reticulum with ribosomes was noted (Supplementary Figure 6B). The ultrastructure of the large nucleus-like structure visible in the FLEC image (Figure 11B) supports a nuclear identity as it had a layered periphery similar to a nuclear envelope (although very thick) and electron dense features akin to nucleoli (Supplementary Figure 6D).

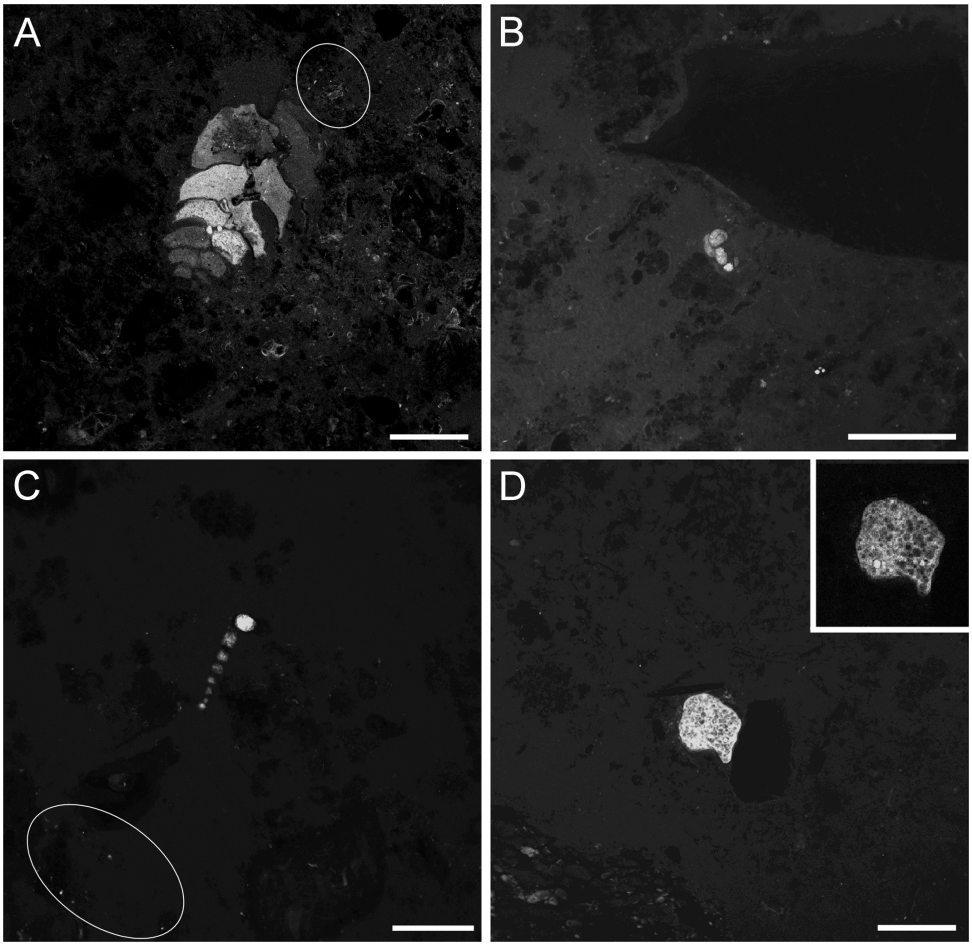

FIGURE 9
LSCM images (z-stacks) of selected foraminifera from chimney-base sediments in FLEC sections. **(A)** Biserial calcareous form, possibly *Euloxostomum pseudobeyrichi* from 4-mm depth in Core 9. **(B)** Multi-chambered enrolled foraminifer (Core 17, 3 mm depth), also likely with a (dissolved) calcium carbonate test. **(C)** Uniserial agglutinated form near the sediment-water interface (Core 19, ~0.5 mm depth). **(D)** Single-chamber agglutinated foraminifer; test sediment grains range from small platelets to silt/sand grain on right (Core 10; 0.5 mm depth). Inset: single scan illustrating typical vacuolar nature of foraminifer's cytoplasm. Bright circular structure is likely nucleus. White ovals in **A**, **C** highlight areas of microbe aggregation. Number of images compiled/distance between images (µm): **(A)**=11/1.4; **(B)**=34/0.5; **(C)** = 20/0.7; **(D)**= 11/0.7; **(D)** Inset = 1 slice. Scales: **(A)** = 200 µm; **(B-D)** = 100 µm.

3.4 Peritrich-targeted Sequencing

Environmental DNA analysis using Peritrich-specific primers revealed that sequences belonging to the Vaginicolidae family of the Vorticellida superfamily were present in four of our six samples dedicated to such analyses (Table 1 Samples A-F; Figure 12). These sequences occurred in the only samples from the chimney wall surfaces (n=2; Samples E, F) as well as in a chimney-base sediment sample (Sample D) and in one sample from non-vent sediments collected inside the caldera (Sample C). Such sequences were absent from one chimney-base sediment sample as well as from a sample collected outside the caldera. The sequences belong to the Vaginicolidae family and were clustered with a *Vaginicola* sp. and *Cothurnia salina*, not with Vorticellidae taxa (Figure 12).

4 Discussion

Our results show that the sedimentary habitat at the base of hydrothermal vent chimneys has a unique and relatively abundant community compared to the other two habitats studied. To put the results in context, we discuss, below, FLEC methodology, which uniquely provides glimpses into sub-mm spatial realities; sedimentological fabric, which demonstrates environmental differences; a synopsis regarding the total

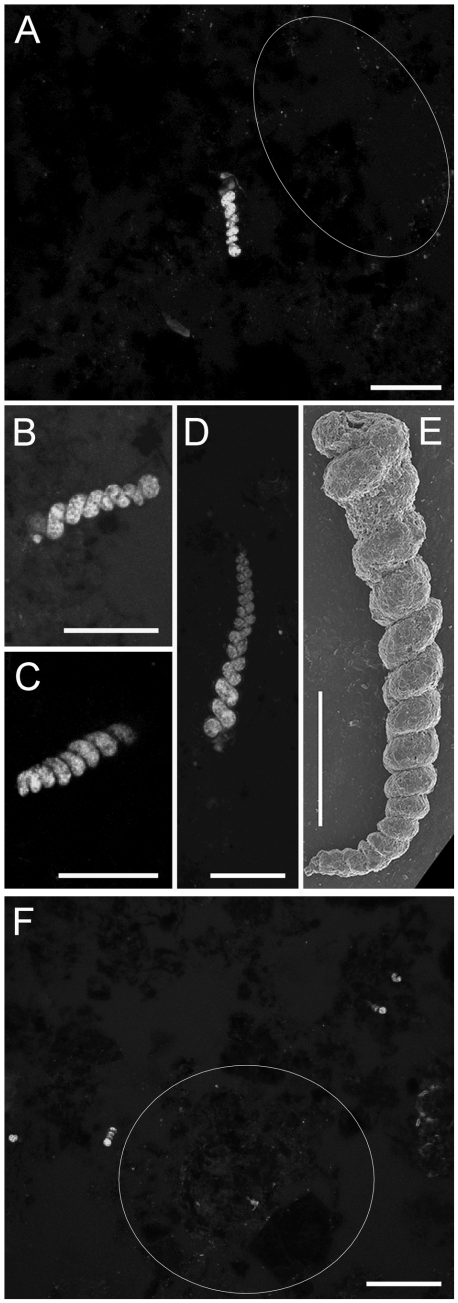

FIGURE 10
Foraminifer *Turritellella* sp., from chimney-base sediments. **(A–D, F)** LSCM images (z-stacks) of specimens from FLEC sections. **(A)** Specimen with aperture up (Core 9; 3 mm depth). **(B, C)** Specimens oriented nearly horizontally (Core 9, 11, respectively, both ~0.5 mm depth). **(D)** Specimen with aperture down (Core 9, 0.5 mm depth). **(E)** SEM micrograph showing spiral growth habit and fine-grained test (0-1-cm interval, SEM core, Myojin-Knoll chimney-base sediments). **(F)** Overview showing four specimens (Core 8, ~1 mm depth). White outlines in **(A, F)** highlight areas of microbe aggregation. Number of images compiled/distance between images (µm): **(A)**=21/0.3; **(B)**=5/0.3; **(C)**= 44/0.3; **(D)**= 8/ 0.3; **(F)** = 37/0.7. Scales: **(A–E)** = 50 µm; **(F)** = 200 µm.

benthos; and separate discussions of the two main eukaryotic benthos: metazoans and protists.

4.1 Methodological advantages

Sediments at the base of hydrothermal vent chimneys are well suited for life-position analyses with FLEC because information can be gleaned about the distributions of organisms on a millimeter or finer scale (Bernhard et al., 2003; First and Hollibaugh, 2010; Bernhard et al., 2013), which may be important given the thin organic-carbon-rich sediment cover over organic-carbon-poor sediments (Figure 10 of Nomaki et al., 2019). Additionally, such sub-mm spatial information provides different perspectives than classical benthic ecology sampling, which typically occurs at scales of 1-cm or more. Furthermore, only enzymatically active organisms label with the FLEC probe (CellTracker™ Green CMFDA), again providing additional insights beyond, for example, DNA sequencing and environmental barcoding.

The slight layering observed in microCT scans of Cores 1 and 2 (e.g., Figure 2A), which were collected outside the caldera, suggest a dearth of bioturbating benthos outside the caldera as well as evidence that the FLEC procedure does not impact sediment fabric and, by inference, organism distributions on the sub-millimeter scale, per prior observations (Bernhard et al., 2003; Bernhard et al., 2013).

4.2 Sediment characteristics

The common occurrence of electron opaque minerals and the unsorted nature of sediments composing the chimney-base cores (Figures 2C-F) indicate that vent chimney debris is a major source to these sediments. Thus, the chimney-base sediments likely receive vent-associated organisms and/or their organic remains. It can be expected, then, that chimney-base sediments support a benthic assemblage that relies, at least partly, on such organic remains from the chimney wall.

Sedimentary TOC values of Myojin Knoll are known to be higher in surface sediments collected at the base of vent chimneys compared to those of sediments far removed from the chimneys and from sediments outside the Myojin Knoll caldera (Nomaki et al., 2019). Generally, the top cm of chimney-base sediments exceeded 0.5% TOC (up to 1.5%) while those of the surface cm of non-vent samples did not exceed 0.5% TOC (Nomaki et al., 2019). Thus, organic carbon values suggest a richer food source near the chimneys; FLEC observations support that perspective because the chimney-base sediments had seemingly more abundant microbial biofilms, interstitial microbes, nanobenthos, and protistan and metazoan meiobenthos compared to samples collected outside the

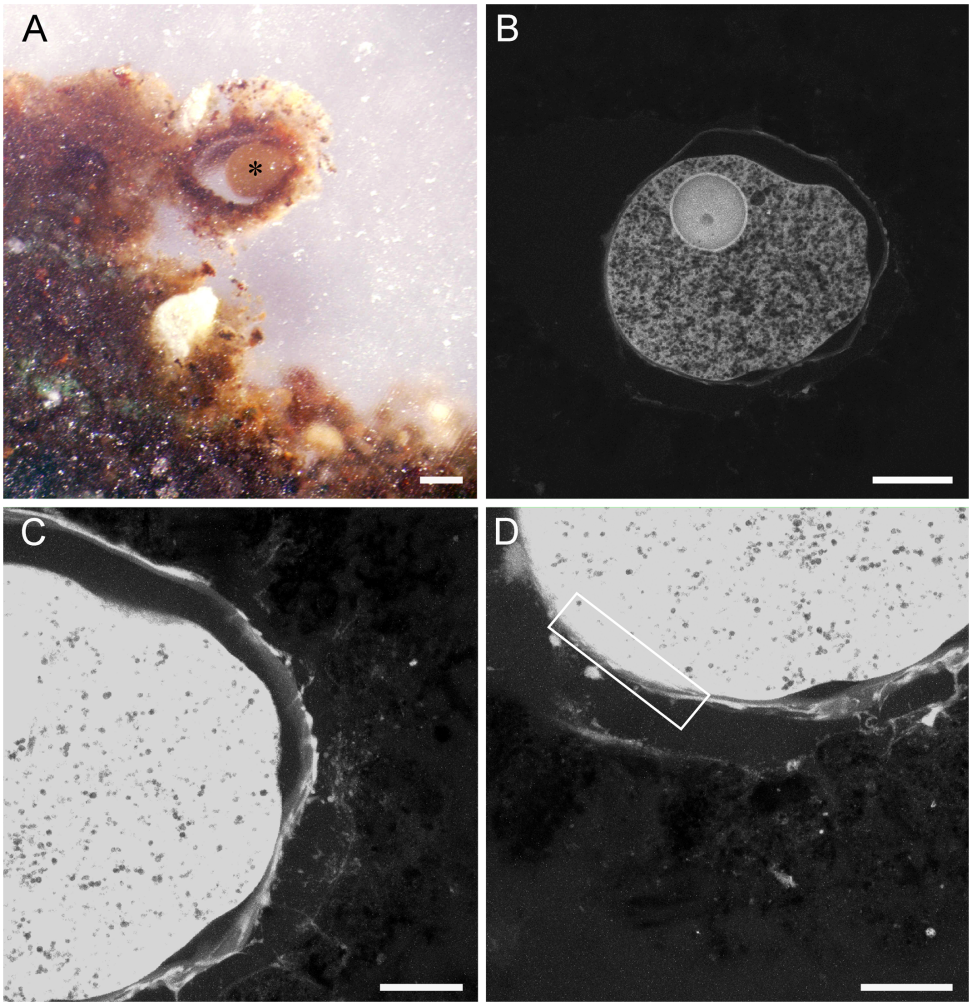

FIGURE 11
Pelosina-like foraminifer from Core 6 (chimney base), preserved with calcium-free seawater. **(A)** Reflected-light micrograph of specimen (*) in FLEC section showing sediment-surface position, in vertical section, inside agglutinated structure. **(B–D)** LSCM images showing specimen of **A**. **(B)** Single-section image showing nucleus and well-preserved cytoplasmic vacuoles. **(C–D)** Z-stacks showing remnant reticulopodia on the exterior of the foraminifer's theca, infiltrating into interior of surrounding test. Cell body is over exposed in **(C, D)** to illustrate the fine reticulopodial remnants. Box in D outlines general area shown in higher magnification in Supplementary Figures 5, 6. Number of images compiled/distance between images (μm): **(B)** = 1 slice; **(C)**= 55/0.3; **(D)**= 57/0.3. Scales: **(A)** = 200 mm; **(B)** = 100 mm; **(C, D)** = 50 mm.

caldera, a trend similar to prior observations regarding metazoan meiofauna abundances from Myojin-Knoll sediment samples examined by conventional community composition analyses (Uejima et al., 2017).

The organisms living near the sediment-water interface likely benefitted from organic materials raining down from the walls of the hydrothermal-vent chimney. This perspective is concordant with our observation that most organisms occurred in the surface ~4 mm (Figure 5), with maximum abundances in the top mm. The possibility that the community occurred subsurface to take advantage of diffuse venting activity or flow was not supported by our observations. It must be remembered, however, that the material in our cores deeper than ~1 cm was often moderately autofluorescent.

4.3 Community differences across habitats

We show that the meiobenthos and nanobenthos are more abundant in cores associated with chimneys than that of caldera cores removed from the chimneys and from cores obtained outside the caldera (Figure 3). Only one chimney-base core (Core 11) had fewer total eukaryote abundances than the most

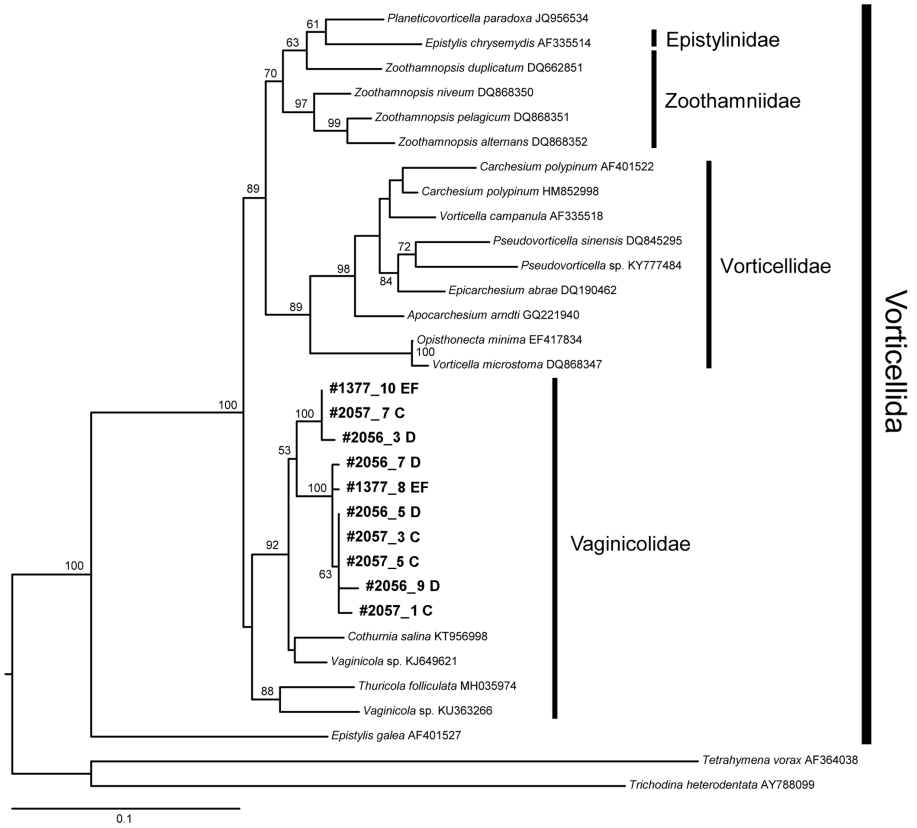

FIGURE 12
Maximum likelihood tree showing the placement of our Vaginicolidae sequences in the context of Vorticellida ciliates. Leaves corresponding to our sequences are in bold. Branch numbers show bootstrap support above 50. The tree is rooted with the distantly related *Tetrahymena vorax*. Scale bar, 0.1% sequence divergence.

abundant non-chimney core (Core 14). Generally, the chimney-base associated cores had two to five times more eukaryotes than non-chimney associated cores.

The chimney-base sedimentary fauna was unique in that the stalked ciliate only occurred in the chimney-base cores (Daimyojin Chimney *via* DNA, smaller chimney *via* FLEC) and the *Turritellella* foraminifer only occurred in the cores from the base of the Daimyojin Chimney. The dominance of ciliates (both stalked and motile) in the cores from the base of the smaller chimney reveals that this community differs in general taxonomic composition compared to that of the Daimyojin Chimney-base cores and non-chimney-associated cores. Such differences suggest a degree of endemism.

4.4 Metazoans

Nematodes were the most commonly observed metazoan, which is consistent with the previous study showing their dominance in all caldera sediments (Uejima et al., 2017). Given nematode counts for Daimyojin Chimney base cores reflect minimum abundances, they were more common in chimney-base sediments compared to non-chimney sediments. Even if a complete nematode was observed (Figure 6A), their critical morphological characteristics cannot be documented with sufficient resolution in FLEC materials to permit sub-phylum identification.

In the sediment in the investigated caldera including around bases of chimneys, benthic copepods (and their nauplii) were the second most abundant metazoan meiofauna after nematodes, supporting prior observations of Uejima et al. (2017). FLEC revealed one putative juvenile copepod (Figure 6D) in one of our chimney-base cores. Its body shape, however, was not that of Harpacticoida that were most frequent in these sediment habitats (Uejima et al., 2017), but rather resembled Cyclopoida or Dirivultidae. Dirivultidae copepods are thought by some to be endemic to hydrothermal vents, always occurring on chimneys or their adjacent hard substrates (Gollner et al., 2010a; Gollner

et al., 2015), which also have been observed with high frequencies on surfaces of vent-chimneys in the study aera (Senokuchi et al., 2018; Uyeno et al., 2018). If this specimen was a dirivultid, and living, as suggested by its fluorescently labeled tissues, our observation expands the known habitat of this copepod to the sedimentary habitat.

Ostracods have been associated with active hydrothermal vents (e.g., Maddocks, 2005; Yasuhara et al., 2018) with some noted to be endemic (Karanovic and Brandão, 2015; Tanaka and Yasuhara, 2016). Our observations suggest that ostracods can inhabit hydrothermal vent chimney-base sediments. One ostracod noted in our FLEC samples likely was a *Thomontocypris* sp., a genus affiliated with reducing environments including hydrothermal vents (Tanaka and Yasuhara, 2016). It is not possible to determine if this specimen belongs to the vent-associated *Thomontocypris shimanagai*, which was described from Myojin-sho, occurring on the chimney walls (Tanaka and Yasuhara, 2016). Another ostracod from our samples likely is in the Cytheroidea superfamily (H. Tanaka, Pers. Comm.), as it somewhat resembled *Xylocythere sarrazinae*, which was described from the Juan de Fuca hydrothermal vent field in the northeast Pacific (Tanaka et al., 2019). While a confident identification is not possible, the observation of a putative rotifer in our non-chimney-base caldera sediments (Supplementary Figure 2B) is sensible given that benthic rotifers sometimes dominate caldera lakes (e.g., Mucschiol and Traunspurger, 2009). To our knowledge, rotifers have not been documented from deep-sea hydrothermal vents (either chimneys or chimney-base sediments) although rotifers were noted in the Hydrate Ridge hydrocarbon seep area of the Eastern Pacific (Sommer et al., 2007). Only additional dedicated sediment sampling will resolve such metazoan identifications and their ecology.

4.5 Protists

Definitive ciliates, which were noted more often in the chimney-associated FLEC samples than the non-chimney associated samples (Supplementary Table 1), varied greatly in shape, morphology and size. Based on morphology, most of the imaged ciliates were motile (Figure 7) but we also noted a considerable population of one "anchored" form (Figure 8). Because ciliates often support endo-and/or ectosymbionts (e.g., Edgcomb et al., 2011; Beinart et al., 2018; Fokin and Serra, 2022), one might expect they would be successful in environments with steep redox boundaries (e.g., Bernhard et al., 2000) including vent habitats (e.g., Kouris et al., 2007). Further ultrastructural analyses to survey for microbial associates of our FLEC ciliates were beyond the scope of this study.

While our morphological and sequence results were inconsistent at the family level of Sessilida peritrich ciliates (i.e., Vorticellidae vs. Vaginicolidae, respectively), our data suggests a degree of endemism in these cryptic vent communities. The stalked ciliate was only noted in cores from the small chimney but sequence results indicate additional occurrence in Daimyojin Chimney base sediments. An association of *Vorticella*-like and Vagicolidae ciliates with marine hydrothermal vent habitats has not been documented in the literature, although one report notes *Vorticella microstoma* occurrence in a Bavarian methane-seep spring with sulfidic conditions, "marine salinity" and mild hydrothermal temperature (Hoque and Fritscher, 2017). Furthermore, a *Vorticella* species living in a steep redoxcline (mangrove peat) has been noted to have chemoautotrophic ectobionts (Vopel et al., 2002) while a *Pseudovorticella* sp. living on submerged leaves in a mangrove lagoon has sulfur-oxidizing ectobionts, suggesting a thiotrophic symbiosis between that host and ectobiont (Grimonprez et al., 2018). This *Pseudovorticella* sp. looks morphologically similar to our *Vorticella*-like species (compare our Figure 8 to their Figures 1,2,5; Grimonprez et al., 2018).

The presence of Vaginicolidae sequences in both chimney-base sediments and in chimney-wall detritus suggests the "*Vorticella*-like" population in our FLEC chimney-base sediment preparations is actually a Vaginicolid and it likely originated from the chimney surface. A chimney-wall origin for our sedimentary Sessilida is supported by the fact that none of those specimens extended directly into overlying bottom waters but instead into pore waters, depending on their attachment point to displaced portions of chimney rock. Because both Vorticellidae and Vaginicolidae are filter feeders (Pepper et al., 2013), typically of suspended bacteria (e.g., Simek et al., 2019), it is likely that this Sessilida peritrich abounds in chimney-wall habitats due to the high production of prokaryotic biomass associated with hydrothermal activity. As noted above, however, it is also possible our *Vorticella*-like species has ectobionts that bolster its ability to live in or close to hydrothermal venting. Specimens of the *Vorticella*-like morphotype did not appear encysted, as is known for some *Vorticella* species (Finley and Lewis, 1960), unless the two stalk-less spherical entities of similar diameter were cysts. If so, they were not dormant as those spheres labeled with CTG, which relies on esterases to impart fluorescence.

To date, very few foraminiferal species have been described as endemic to hydrothermal vents. For example, *Abyssotherma pacifica* encrusts on hard substrates near venting fluids of the East Pacific Rise (Brönnimann et al., 1989; Lee et al., 1991). Because our multi-chambered agglutinated trochospiral foraminifers (i.e., generally morphologically similar to *A.*

pacifica; Figure 9B, Supplementary Figure 4A) were in "soft" sediment, we infer that none are *A. pacifica*. Our materials did not reveal any individuals similar to any other possible vent endemic foraminifers (e.g., *Ropostrum amuletum*, Jonasson and Schroeder-Adams, 1996).

The common foraminifer morphotype we observed, tentatively identified as a species of *Turritellella*, occurred in sufficient numbers to comment on its distribution, ecology, and possible species affiliation. Our *Turritellella* was only found in the cores collected at the base of Daimyojin chimney (Cores 8, 9, 11). This *Turritellella* occurred in relatively high abundances (as high as 11.3 individuals cm^{-3}) for such bathyal water depths (1267m), being comparable to the five most abundant foraminifer species from two non-seep sites in the eastern Pacific [Monterey Bay, 906 m and 1003 m: *Bolivina spissa*, 11.0 specimens cm^{-3}; *Buliminella tenuata*, 10.4 specimens cm^{-3}; *Uvigerina peregrina*, 10.4 specimens cm^{-3}; *Phthanotrochus arcanus*, 18.1 specimenscm^{-3}; *Textularia* sp. 9.6 specimens cm^{-3} (Bernhard et al., 2010)], as determined by the viability assay of adenosine triphosphate content (i.e., [ATP]; Delaca, 1986).

Turritellella is not a common foraminiferal genus, with only three described extant species. Our *Turritellella* specimens appear similar to *T. shoneana*, which is documented episodically in Scandinavian fjords and the Antarctic, as well as in locales around Japan and New Zealand (Hayward et al., 2022). No published reports indicate a link between *Turritellella* species and hydrothermal vents or other "extreme" (e.g., reducing) habitats. The species may tolerate hypoxia, given it occurred as deep as ~3 mm in our samples. Additional dedicated sampling is necessary to determine if this morphologically distinct agglutinated foraminifer is endemic to the sediments at the base of hydrothermal vent chimneys.

Some agglutinated single-chambered spherical foraminifera similar in appearance to the genus *Pelosina* (Brady, 1879) were noted in our FLEC materials (Figures 9D, 11A). Our ultrastructural analyses suggest that the fluorescent *Pelosina* specimen of Figure 11A was living and active at the time of fixation, given the overall nature of the vacuolated cytoplasm and certain intact organelles (Golgi, endoplasmic reticulum with ribosomes, microtubules, nucleus; Supplementary Figures 5, 6). Remnant reticulopods and CTG labeling support the assertion that this putative *Pelosina* was active. The considerable abundance of Golgi in our *Pelosina* specimen examined with TEM bolsters the assertion of activity because Golgi transport proteins throughout the cell. While the double membranes and cristae of the *Pelosina* mitochondria were not well preserved, it should be noted that these preparations are not ideally processed for TEM due to the objective of FLEC life position analyses. In particular, materials processed for FLEC were not osmicated, which emphasizes biological membranes, before embedding as usual for TEM (e.g., Bernhard et al., 2000).

While many hydrothermal vent-associated mega- and macrofauna (e.g., tube worms; mussels) have endosymbionts (Cavanaugh et al., 1981; Sogin et al., 2021), there was no evidence of endobionts in the *Pelosina* cell body. Such an observation is not surprising given the active venting was many meters above the sampled sediments. The $\delta^{15}N$ values of *Pelosina* sp. from Myojin Knoll were quite elevated (~19‰; Nomaki et al., 2019), being much higher than surrounding sediments, indicating perhaps that this foraminifer denitrifies, as suggested by others for non-vent foraminifera (e.g., Nomaki et al., 2015; Jeffreys et al., 2015) and as known for other foraminifera from non-vent oxygen-depleted habitats (e.g., Risgaard-Petersen et al., 2006; Bernhard et al., 2012; Gomaa et al., 2021). Additional studies are required to determine if this *Pelosina* denitrifies and/or is exclusive to chimney-base sediments, as our data and that of Nomaki et al. (2019) suggest.

The theca of the *Pelosina*-like specimen (Supplementary Figures 5A-C) appeared somewhat similar to thecae of *Astrammina rara* and *A. triangularis*, which are in the same order as *Pelosina* (i.e., Astrorhizida), in having a fibrous fabric and a tripartite exterior layer (Supplementary Figures 5B,D) (Bowser et al., 1995; Bowser and Travis, 2002) although it lacked a well-developed vesicular layer and herring-bone pattern, as known for *A. rara* (Bowser et al., 1995). The Astrorhizida belong to what is considered the basal or most primitive foraminiferal group (i.e., Monothalamea or monothalamids; (e.g., Pawlowski et al., 2003; Sierra et al., 2022).

The occurrence of abundant living basal Monothalamea foraminifera as well as the derived Tubothalamea (i.e., *Turritellella*) in our seep-associated sediment samples could be interpreted as evidence that these vent-associated sediments may have been a nexus for early foraminiferal diversification. This perspective is supported by observations of additional Tubothalamea and Monothalamea (e.g., *Jaculella acuta*; Jonasson and Schroeder-Adams, 1996; McCloskey, 2009), as well as the more common Globothalamea [i.e., multichambered forms such as *A. pacifica* (Lee et al., 1991; Gollner et al., 2007)] although those studies and others (Gollner et al., 2010b) unfortunately did not establish viability of their foraminifers.

5 Conclusions

Meiofauna and nanobiota inhabited sediments occurring at the base of two hydrothermal-vent chimneys in the Western North Pacific, with the community concentrated in the surface half cm. The prevalence of specimens near the sediment-water interface suggests they utilize organics raining from the towering chimney rather than obtain reduced compounds deeper in sediments, through the chimney wall. Differences in taxonomic composition, abundances, and dominance suggest that the chimney-base community is unique and more abundant compared to non-chimney associated eukaryotic communities. As such, this habitat and its community are deserving of detailed study. Such investigations should target the unusual chimney-

base fauna (i.e., *Turritellella* foraminifer and stalked ciliate), as well as other protists, to determine their biogeography and physiology. Furthermore, the communities of additional chimneys deserve focused study.

Data availability statement

The dataset presented in this study can be found in online repositories. The names of the repository/repositories and accession number(s) can be found below: https://www.ncbi.nlm.nih.gov/genbank/, LC723767- LC723776.

Author contributions

MS, HN and JB conceived of the project and obtained the funding, HN, JB, and MS collected the samples, JB, HN, TS, MT, AE, AY, and KK performed analyses, JMB, HN, and MS interpreted the data, JB and HN wrote the majority of the manuscript. All authors provided manuscript comments and approved of the final version.

Funding

Supported by a grant from the Japan Society for the Promotion of Science (JSPS) Grants-in-Aid for Scientific Research (KAKENHI) program (grant numbers JP26440246 and JP19H03305). JB's support is also acknowledged: the Invitational Fellowships for Research in Japan funded by JSPS, Stanley W. Watson Senior Scientist Chair, and *The Investment in Science Program* at WHOI.

Acknowledgments

We thank the Captains, Crews and onboard scientists of the R/V *Natsushima* and *Hyperdolphin* ROV Team for facilitating sample collections; Kaya Oda for her help on *Turritellella* sp. isolation from the sediments for SEM imaging; Drs. Chong Chen, Hiromi K. Watanabe, and Hayato Tanaka for their comments on the identities of some metazoan images. We thank the two reviewers for their comments on an earlier version of the manuscript.

Conflict of interest

The authors declare that the research was conducted in the absence of any commercial or financial relationships that could be construed as a potential conflict of interest.

Publisher's note

Supplementary material

The Supplementary Material for this article can be found online at: https://www.frontiersin.org/articles/10.3389/fmars.2022.1033381/full#supplementary-material

References

Beinart, R. A., Beaudoin, D. J., Bernhard, J. M., and Edgcomb, V. P. (2018). Insights into the metabolic functioning of a multipartner ciliate symbiosis from oxygen-depleted sediments. *Mol. Ecol.* 27, 1794–1807. doi: 10.1111/mec.14465

Bernhard, J. M., and Bowser, S. S. (1996). Novel epifluorescence microscopy method to determine life position of foraminifera in sediments. *J. Of Micropalaeontol.* 15, 68–68. doi: 10.1144/jm.15.1.68

Bernhard, J. M., and Buck, K. R. (2004). "Eukaryotes of the cariaco, soledad, and Santa Barbara Basins: Protists and metazoans associated with deep-water marine sulfide-oxidizing microbial mats and their possible effects on the geologic record," in Sulfur biogeochemistry– past and present. Eds. J. P. Amend, K. J. Edwards and T. W. Lyons *GSA Special Paper* GSA headquartered, Denver, Colorado, USA 379, pp 35–47. doi: 10.1130/0-8137-2379-5.35

Bernhard, J. M., Buck, K. R., Farmer, M. A., and Bowser, S. S. (2000). The Santa Barbara Basin is a symbiosis oasis. *Nature* 403, 77–80. doi: 10.1038/47476

Bernhard, J. M., Casciotti, K. L., Mcilvin, M. R., Beaudoin, D. J., Visscher, P. T., and Edgcomb, V. P. (2012). Potential importance of physiologically diverse benthic foraminifera in sedimentary nitrate storage and respiration. *J. of Geophysical Research-Biogeosciences* 117. doi: 10.1029/2012jg001949

Bernhard, J. M., Edgcomb, V. P., Visscher, P. T., Mcintyre-Wressnig, A., Summons, R., Bouxsein, M. L., et al. (2013). Insights into foraminiferal influences on microfabrics of microbialites At highborne cay, Bahamas. *Proc. of Natl. Acad. of Sci. of United States of America* 110, 9830–9834. doi: 10.1073/pnas.1221721110

Bernhard, J. M., Habura, A., and Bowser, S. S. (2006). An endobiont-bearing allogromiid from the Santa Barbara Basin: Implications for the early diversification of foraminifera. *J. Of Geophysical Research-Biogeosciences* 111, G03002. doi: 10.1029/2005JG000158

Bernhard, J. M., Martin, J. B., and Rathburn, A. E. (2010). Combined carbonate carbon isotopic and cellular ultrastructural studies of individual benthic foraminifera: 2. toward an understanding of apparent disequilibrium in hydrocarbon seeps. *Paleoceanography* 25, Pa4206. doi: 10.1029/2010PA001930

Bernhard, J. M., and Richardson, E. A. (2014). "FLEC-TEM: Using microscopy to correlate ultrastructure with life position of infaunal foraminifera," in *Approaches to study living foraminifera: Collection, maintenance and experimentation*. Eds. H. Kitazato and J. M. Bernhard (Tokyo: Springer Japan). doi: 10.1007/978-4-431-54388-6_7

Bernhard, J. M., Visscher, P. T., and Bowser, S. S. (2003). Submillimeter life positions of bacteria, protists, and metazoans in laminated sediments of the Santa Barbara Basin. *Limnol. And Oceanogr.* 48, 813–828. doi: 10.4319/lo.2003.48.2.0813

Bowser, S. S., Gooday, A. J., Alexander, S. P., and Bernhard, J. M. (1995). Larger agglutinated foraminifera of McMurdo Sound, Antarctica: Are *Astrammina rara* and *Notodendrodes antarctikos* allogromiids incognito? *Mar. Micropaleontol.* 26, 75–88. doi: 10.1016/0377-8398(95)00024-0

Bowser, S. S., and Travis, J. L. (2002). Reticulopodia: Structural and behavioral basis for the suprageneric placement of granuloreticulosan protists. *J. Of Foraminiferal Res.* 32, 440–447. doi: 10.2113/0320440

Brady, H. B. (1879). Notes on some of the reticularian rhizopoda of the "*Challenger*" expedition; part i. on new or little known arenaceous types. *Q. J. Of Microscopical Sci.* 19, 20–67. doi: 10.1242/jcs.s2-19.73.20

Brönnimann, P., Van Dover, C. L., and Whittaker, J. E. (1989). *Abyssotherma pacifica*, n. gen., n. sp., a recent remaneicid (Foraminiferida, remaneicacea) from the East Pacific Rise. *Micropaleontology* 35, 142–149. doi: 10.2307/1485465

Cavanaugh, C. M., Gardiner, S. L., Jones, M. L., Jannasch, H. W., and Waterbury, J. B. (1981). Prokaryotic cells in the hydrothermal vent tube worm *Riftia pachyptila* Jones: Possible chemoautotrophic symbionts. *Science* 213, 340–342. doi: 10.1126/science.213.4505.340

Chen, C., Watanabe, H. K., and Sasaki, T. (2019). Four new deep-Sea provannid snails (Gastropoda: Abyssochrysoidea) discovered from hydrocarbon seep and hydrothermal vents in Japan. *R. Soc. Open Sci.* 6, 190393. doi: 10.1098/rsos.190393

Coyne, K. J., Countway, P. D., Pilditch, C. A., Lee, C. K., Caron, D. A., and C., C. S. (2013). Diversity and distributional patterns of ciliates in Guaymas Basin hydrothermal vent sediments. *J. Of Eukaryotic Microbiol.* 60, 433–447. doi: 10.1111/jeu.12051

Delaca, T. E. (1986). Determination of benthic rhizopod biomass using ATP analysis. *J. Of Foraminiferal Res.* 16, 285–292. doi: 10.2113/gsjfr.16.4.285

Edgcomb, V. P., Kysela, D. T., Teske, A., De Vera Gomez, A., and Sogin, M. L. (2002). Benthic eukaryotic diversity in the Guaymas Basin hydrothermal vent environment. *Proc. Of Natl. Acad. Of Sci.* 99, 7658–7662. doi: 10.1073/pnas.062186399

Edgcomb, V. P., Leadbetter, E. R., Bourland, W., Beaudoin, D., and Bernhard, J. M. (2011). Structured multiple endosymbiosis of bacteria and archaea in a ciliate from marine sulfidic sediments: A survival mechanism in low oxygen, sulfidic sediments? *Front. In Microbiol.* 2, Art. doi: 10.3389/fmicb.2011.00055

Finley, H. E., and Lewis, A. C. (1960). Observations on excystment and encystment of *Vorticella microstoma*. *J. Of Protozool.* 7, 347–351. doi: 10.1111/j.1550-7408.1960.tb05981.x

First, M. R., and Hollibaugh, J. T. (2010). Diel depth distributions of microbenthos in tidal creek sediments: High resolution mapping in fluorescently labeled embedded cores. *Hydrobiologia* 655, 149–158. doi: 10.1007/s10750-010-0417-2

Fokin, S. I., and Serra, V. (2022). Bacterial symbiosis in ciliates (Alveolata, ciliophora): Roads traveled and those still to be taken. *J. Of Eukaryotic Microbiol.* 69, E12886. doi: 10.1111/jeu.12886

Frankel, L. (1970). A technique for investigating microorganism associations. *J. Of Paleontol.* 44, 575–577. http://jstor.org/stable/1302595

Gollner, S., Govenar, B., Fisher, C. R., and Bright, M. (2015). Size matters at deep-sea hydrothermal vents: Different diversity and habitat fidelity patterns of meio- and macrofauna. *Mar. Ecol. Prog. Ser.* 520, 57–66. doi: 10.3354/meps11078

Gollner, S., Ivanenko, V. N., Arbizu, P. M., and Bright, M. (2010a). Advances in taxonomy, ecology, and biogeography of dirivultidae (Copepoda) associated with chemosynthetic environments in the deep Sea. *PloS One* 5, E9801. doi: 10.1371/journal.pone.0009801

Gollner, S., Riemer, B., Martínez Arbizu, P., Le Bris, N., and Bright, M. (2010b). Diversity of meiofauna from the 9°50′N East Pacific Rise across a gradient of hydrothermal fluid emissions. *PloS One* 5, E12321. doi: 10.1371/journal.pone.0012321

Gollner, S., Zekely, J., Govenar, B., Le Bris, N., Nemeschkal, H. L., R., F. C., et al. (2007). Tubeworm-associated permanent meiobenthic communities from two chemically different hydrothermal vent sites on the East Pacific Rise. *Mar. Ecol. Prog. Ser.* 337, 39–49. doi: 10.3354/meps337039

Gomaa, F., Utter, D. R., Powers, C., Beaudoin, D. J., Edgcomb, V. P., Filipsson, H. L., et al. (2021). Multiple integrated metabolic strategies allow foraminiferan protists to thrive in anoxic marine sediments. *Sci. Adv.* 7, Eabf1586. doi: 10.1126/sciadv.abf1586

Gooday, A. J. (2002). Organic-walled allogromiids: Aspects of their occurrence, diversity and ecology in marine habitats. *J. Foraminiferal Res.* 32, 384–399. doi: 10.2113/0320384

Gouy, M., Guindon, S., and Gascuel, O. (2010). Seaview version 4: A multiplatform graphical user interface for sequence alignment and phylogenetic tree building. *Mol. Biol. And Evol.* 27, 221–224. doi: 10.1093/molbev/msp259

Grimonprez, A., Molza, A., Laurent, M. C. Z., Mansot, J.-L., and Gros, O. (2018). Thioautotrophic ectosymbiosis in *Pseudovorticella* sp., a peritrich ciliate species colonizing wood falls in marine mangrove. *Eur. J. Of Protistol.* 62, 43–55. doi: 10.1016/j.ejop.2017.11.002

Hayward, B., Le Coze, F., Vachard, D., and Gross, O. (2022)World foraminifera database. In: *Turritellella shoneana (Siddal)*. Available at: https://Www.Marinespecies.Org/Aphia.Php?P=Taxdetails&Id=113835 (Accessed 08/02 2022).

Höglund, H. G. (1947). *Foraminifera in the gullmar fjord and the skagerrak* (Uppsala: Zoologiska Bidrag Från Uppsala).

Honsho, C., Ura, T., Kim, K., and Asada, A. (2016). Postcaldera volcanism and hydrothermal activity revealed by autonomous underwater vehicle surveys in Myojin Knoll Caldera, Izu-Ogasawara Arc. *J. Of Geophysical Research-Solid Earth* 121, 4085–4102. doi: 10.1002/2016JB012971

Hoque, E., and Fritscher, J. (2017). Ecology, adaptation, and function of methane-sulfidic spring water biofilm microorganisms, including a strain of anaerobic fungus *Mucor hiemalis*. *Microbiol. Open* 6, E483. doi: 10.1002/mbo3.483

Iizasa, K., Fiske, R. S., Ishizuka, O., Yuasa, M., Hashimoto, J., Ishibashi, J., et al. (1999). A Kuroko-type polymetallic sulfide deposit in a submarine silicic caldera. *Science* 283, 975–977. doi: 10.1126/science.283.5404.975

Jeffreys, R. M., Fisher, E. H., Gooday, A. J., Larkin, K. E., Billett, D. S. M., and Wolff, G. A. (2015). The trophic and metabolic pathways of foraminifera in the Arabian Sea: Evidence from cellular stable isotopes. *Biogeosciences* 12, 1781–1797. doi: 10.5194/bg-12-1781-2015

Jonasson, K. E., and Schroeder-Adams, C. J. (1996). Encrusting agglutinated foraminifera on indurated sediment at a hydrothermal venting area on the Juan de Fuca Ridge, northeast Pacific Ocean. *J. Of Foraminiferal Res.* 26, 137–149. doi: 10.2113/gsjfr.26.2.137

Karanovic, I., and Brandão, S. N. (2015). Biogeography of deep-sea wood fall, cold seep and hydrothermal vent ostracoda (Crustacea), with the description of a new family and a taxonomic key to living cytheroidea. *Deep-Sea Res. I* 111, 76–94. doi: 10.1016/j.dsr2.2014.09.008

Katoh, K., and Standley, D. M. (2013). Mafft multiple sequence alignment software version 7: Improvements in performance and usability. *Mol. Biol. And Evol.* 30, 772–780. doi: 10.1093/molbev/mst010

Koito, T., Saitou, S., Nagasaki, T., Yamagami, S., Yamanaka, T., Okamura, K., et al. (2018). Taurine-related compounds and other free amino acids in deep-sea hydrothermal vent and non-vent invertebrates. *Mar. Biol.* 165, 183. doi: 10.1007/s00227-018-3442-8

Kouris, A., Juniper, S. K., Frébourg, G., and Gaill, F. (2007). Protozoan bacterial symbiosis in a deep-sea hydrothermal vent folliculinid ciliate (*Folliculinopsis* sp.) from the Juan de Fuca Ridge. *Mar. Ecol.* 28, 63–71. doi: 10.1111/j.1439-0485.2006.00118.x

Lee, J. J., Anderson, O. R., Karim, B., and Beri, J. (1991). Additional insight into the structure and biology of *Abyssotherma pacifica* (Brönnimann, van Dover and Whittaker) from the East Pacific Rise. *Micropaleontology* 37, 303–312. doi: 10.2307/1485892

Liu, X. H., and Gong, J. (2012). Revealing the diversity and quantity of peritrich ciliates in environmental samples using specific primer-based PCR and quantitative PCR. *Microbes And Environments* 27, 497–503. doi: 10.1264/jsme2.ME12056

López-García, P., Philippe, H., Gail, F., and Moreira, D. (2003). Autochthonous eukaryotic diversity in hydrothermal sediment and experimental microcolonizers At the mid-Atlantic Ridge. *Proc. Of Natl. Acad. Of Sci.* 100, 697–702. doi: 10.1073/pnas.0235779100

Maddocks, R. F. (2005). Three new species of podocopid ostracoda from hydrothermal vent fields At 9°50'n on the East Pacific Rise. *Micropaleontology* 51, 345–372. doi: 10.2113/gsmicropal.51.5.345

McCloskey, B. J. (2009). *Foraminiferal responses to arsenic in a shallow-water hydrothermal system in paua new Guinea and in the laboratory* (St. Petersburg, Florida: University of South Florida). PhD Dissertation.

Medlin, L., Elwood, H. J., Stickel, S., and Sogin, M. L. (1988). The characterization of enzymatically amplified eukaryotic 16S-like rRNA-coding regions. *Gene* 71, 491–499. doi: 10.1016/0378-1119(88)90066-2

Meisterfeld, R., Holzmann, M., and Pawlowski, J. (2001). Morphological and molecular characterization of a new terrestrial allogromiid apecies: *Edaphoallogromia australica* gen. et spec. nov. (Foraminifera) from northern Queensland (Australia). *Protist* 152, 185–192. doi: 10.1078/1434-4610-00058

Mucschiol, D., and Traunspurger, W. (2009). Life At the extreme: Meiofauna from three unexplored lakes in the caldera of the Cerro Azul volcano, Galapagos Islands, Ecuador. *Aquat. Ecol.* 43, 235–248. doi: 10.1007/s10452-008-9202-y

Murdock, S. A., and Juniper, S. K. (2019). Hydrothermal vent protistan distribution along the Mariana Arc suggests vent endemics may be rare and novel. *Environ. Microbiol.* 21, 3796–3815. doi: 10.1111/1462-2920.14729

Nguyen, L. T., Schmidt, H. A., Von Haeseler, A., and Minh, B. Q. (2015). IQ-TREE: A fast and effective stochastic algorithm for estimating maximum-likelihood phylogenies. *Mol. Biol. And Evol.* 32, 268–274. doi: 10.1093/molbev/msu300

Nomaki, H., Chikaraishi, Y., Tsuchiya, M., Toyofuku, T., Suga, H., Sasaki, Y., et al. (2015). Variation in the nitrogen isotopic composition of amino acids in

benthic foraminifera: Implications for their adaptation to oxygen-depleted environments. *Limnol. And Oceanogr.* 60, 1906–1916. doi: 10.1002/lno.10140

Nomaki, H., Ogawa, N. O., Ohkouchi, N., Suga, H., Toyofuku, T., Shimanaga, M., et al. (2008). Benthic foraminifera as trophic links between phytodetritus and benthic metazoans: Carbon and nitrogen isotopic evidence. *Mar. Ecol. Prog. Ser.* 357, 153–164. doi: 10.3354/meps07309

Nomaki, H., Uejima, Y., Ogawa, N. O., Yamane, M., Watanabe, H. K., Senokuchi, R., et al. (2019). Nutritional sources of meio- and macrofauna at hydrothermal vents and adjacent areas: Natural-abundance radiocarbon and stable isotope analyses. *Mar. Ecol. Prog. Ser.* 622, 49–65. doi: 10.3354/meps13053

Nozaki, T., Ishibashi, J.-I., Shimada, K., Nagase, T., Takaya, Y., Kato, Y., et al. (2016). Rapid growth of mineral deposits at artificial seafloor hydrothermal vents. *Sci. Rep.* 6, 22163. doi: 10.1038/srep22163

Pawlowski, J., Holzmann, M., Berney, C., Fahrni, J., Gooday, A. J., Cedhagen, T., et al. (2003). The evolution of early foraminifera. *Proc. Of Natl. Acad. Of Sci. Of United States Of America* 100, 11494–11498. doi: 10.1073/pnas.2035132100

Pepper, R. E., Roper, M., Ryu, S., Matsumoto, N., Nagai, M., and Stone, H. A. (2013). A new angle on microscopic suspension feeders near boundaries. *Biophys. J.* 105, 1796–1804. doi: 10.1016/j.bpj.2013.08.029

Risgaard-Petersen, N., Langezaal, A. M., Ingvardsen, S., Schmid, M. C., Jetten, M. S. M., Op Den Camp, H. J. M., et al. (2006). Evidence for complete denitrification in a benthic foraminifer. *Nature* 443, 93–96. doi: 10.1038/nature05070

Sarrazin, J., Legendre, P., De Busserolles, F., Fabri, M.-C., Giulini, K., Ivanenko, V., et al. (2015). Biodiversity patterns, environmental drivers and indicator species on a high-temperature hydrothermal edifice, Mid-Atlantic Ridge. *Deep-Sea Res. Ii* 121, 177–192. doi: 10.1016/j.dsr2.2015.04.013

Sasaki, T., Geiger, D. L., and Okutani, T. (2010). A new species of *Anatoma* (Vetigastropoda: Anatomidae) from a hydrothermal vent field in Myojin Knoll caldera, Izu-Ogasawara Arc, Japan. *Veliger* 51, 63–75.

Senokuchi, R., Nomaki, H., Watanabe, H. K., Kitahashi, T., Ogawa, N. O., and Shimanaga, M. (2018). Chemoautotrophic food availability influences copepod assemblage composition at deep hydrothermal vent sites within sea knoll calderas in the northwestern Pacific. *Mar. Ecol. Prog. Ser.* 607, 37–51. doi: 10.3354/meps12804

Setoguchi, Y., Nomaki, H., Kitahashi, T., Watanabe, H., Inoue, K., Ogawa, N. O., et al. (2014). Nematode community composition in hydrothermal vent and adjacent non-vent fields around Myojin Knoll, a seamount on the Izu-Ogasawara Arc in the Western North Pacific Ocean. *Mar. Biol.* 161, 1775–1785. doi: 10.1007/s00227-014-2460-4

Siddall, J. D. (1878). The foraminifera of the River Dee. *Proc. Of Chester Soc. Of Natural Sci.* 2, 42–56.

Sierra, R., Mauffrey, F., Cruz, J., Holzmann, M., Gooday, A. J., Maurer-Alcalá, X., et al. (2022). Taxon-rich transcriptomics supports higher-level phylogeny and major evolutionary trends in foraminifera. *Mol. Phylogenet. And Evol.* 174, 107546. doi: 10.1016/j.ympev.2022.107546

Simek, K., Grujcic, V., Nedoma, J., Jezberov, J., Sorf, M., Matousu, A., et al. (2019). Microbial food webs in hypertrophic fishponds: Omnivorous ciliate taxa are major protistan bacterivores. *Limnol. And Oceanogr.* 64, 2295–2309. doi: 10.1002/lno.11260

Sogin, M. E., Kleiner, M., Borowski, C., Gruber-Vodicka, H. R., and Dubilier, N. (2021). Life in the dark: Phylogenetic and physiological diversity of chemosynthetic symbioses. *Annu. Rev. Of Microbiol.* 75, 695–718. doi: 10.1146/annurev-micro-051021-123130

Sommer, S., Gutzmann, E., and Pfannkuche, O. (2007). Sediments hosting gas hydrates: Oases for metazoan meiofauna. *Mar. Ecology-Progress Ser.* 337, 27–37. doi: 10.3354/meps337027

Tanaka, H., Lelièvre, Y., and Yasuhara, M. (2019). *Xylocythere sarrazinae*, a new cytherurid ostracod (Crustacea) from a hydrothermal vent field on the Juan de Fuca Ridge, northeast Pacific Ocean, and its phylogenetic position within Cytheroidea. *Mar. Biodiversity* 49, 2571–2586. doi: 10.1007/s12526-019-00987-3

Tanaka, H., and Yasuhara, M. (2016). A new deep-Sea hydrothermal vent species of ostracoda (Crustacea) from the Western pacific: Implications for adaptation, endemism, and dispersal of ostracodes in chemosynthetic systems. *Zoological Sci.* 33, 555–565. doi: 10.2108/zs160079

Tsunogai, U., Yoshida, N., Ishibashi, J., and Gamo, T. (2000). Carbon isotopic distribution of methane in deep-sea hydrothermal plume, Myojin Knoll Caldera, Izu-Bonin Arc: Implications for microbial methane oxidation in the oceans and applications to heat flux estimation. *Geochimica et Cosmochimica Acta* 64, 2439–2452. doi: 10.1016/S0016-7037(00)00374-4

Uejima, Y., Nomaki, H., Senokuchi, R., Setoguchi, Y., Kitahashi, T., Watanabe, H. K., et al. (2017). Meiofaunal communities in hydrothermal vent and proximate non-vent habitats around neighboring seamounts on the Izu-Ogawasara Arc, western North Pacific Ocean. *Mar. Biol.* 164, 183. doi: 10.1007/s00227-017-3218-6

Uyeno, D., Watanabe, H. K., and Shimanaga, M. (2018). A new dirivultid copepod (Siphonostomatoida) from hydrothermal vent fields of the Izu-Bonin Arc in the North Pacific Ocean. *2018* 4415, 9. doi: 10.11646/zootaxa.4415.2.8

Van Dover, C. L. (2000). *The ecology of deep-Sea hydrothermal vents* (Princeton: Priceton University Press). doi: 10.1515/9780691239477

Vanreusel, A., Den Bossche, V., and Thiermann, F. (1997). Free-living marine nematodes from hydrothermal sediments: Similarities with communities from diverse reduced habitats. *Mar. Ecol. Prog. Ser.* 157, 207–219. doi: 10.3354/meps157207

Vopel, K., Reick, C. H., Arlt, G., Pöhn, M., and Ott, J. A. (2002). Flow microenvironment of two marine peritrich ciliates with ectobiotic chemoautotrophic bacteria. *Aquat. Microbial Ecol.* 29, 19–28. doi: 10.3354/ame029019

Watanabe, H. K., Shigeno, S., Fujikura, K., Matsui, T., Kato, S., and Yamamoto, H. (2019). Faunal composition of deep-sea hydrothermal vent fields on the Izu-Bonin-Mariana Arc, nortwestern Pacific. *Deep-sea Res. I* 149, 103050. doi: 10.1016/j.dsr.2019.05.010

Watling, L. (1988). Small-scale features of marine sediments and their importance to the study of deposit-feeding. *Mar. Ecol. Prog. Ser.* 47, 135–144. doi: 10.3354/meps047135

Yasuhara, M., Sztybor, K., Rasmussen, T. L., Okahashi, H., Sato, R., and Tanaka, H. (2018). Cold-seep ostracods from the Western Svalbard margin: Direct palaeo-indicator for methane seepage? *J. Of Micropalaeontol.* 37, 139–148. doi: 10.5194/jm-37-139-2018

Yorisue, T., Chan, B. K. K., Kado, R., Watanabe, H., Inoue, K., Kojima, S., et al. (2016). On the morphology of antennular sensory and attachment organs in cypris larvae of the deep-sea vent/seep barnacles, *Ashinkailepas* and *Neoverruca*. *J. Of Morphol.* 277, 594–602. doi: 10.1002/jmor.20522

Zekely, J., Gollner, S., Van Dover, C., Govenar, B., Le Bris, N., Nemeschkal, H., et al. (2006a). Nematode communities associated with tubeworm and mussel aggregations on the East Pacific Rise. *Cahiers Biologie Mar.* 47, 477–482.

Zekely, J., Van Dover, C. L., Nemeschkal, H. L., and Bright, M. (2006b). Hydrothermal vent meiobenthos associated with mytilid mussel aggregations from the Mid-Atlantic Ridge and the East Pacific Rise. *Deep-Sea Res. I* 53, 1363–1378. doi: 10.1016/j.dsr.2006.05.010

Zeppilli, D., Bellec, L., Cambon-Bonavita, M.-A., Decraemer, W., Fontaneto, D., Fuchs, S., et al. (2019). Ecology and trophic role of *Oncholaimus dyvae* sp. nov. (Nematoda: Oncholaimidae) from the Lucky Strike hydrothermal vent field (Mid-Atlantic Ridge). *BMC Zool.* 4, 6. doi: 10.1186/s40850-019-0044-y

Zeppilli, D., Bongiorni, L., Santos, R. S., and Vanreusel, A. (2014). Changes in nematode communities in different physiographic sites of the Condor Seamount (North-East Atlantic Ocean) and adjacent sediments. *PloS One* 9, E115601. doi: 10.1371/journal.pone.0115601

Zeppilli, D., Leduc, D., Fontanier, C., Fontaneto, D., Fuchs, S., Gooday, A. J., et al. (2018). Characteristics of meiofauna in extreme marine ecosystems: A review. *Mar. Biodiversity* 48, 35–71. doi: 10.1007/s12526-017-0815-z